Molecular characterization of gaseous and particulate oxygenated compounds at a remote site in Cape Corsica in the western Mediterranean basin.

Vincent Michoud[1], Elise Hallemans[1,2], Laura Chiappini[2,†], Eva Leoz-Garziandia[2], Aurélie Colomb[3], Sébastien Dusanter[4], Isabelle Fronval[4], François Gheusi[5], Jean-Luc Jaffrezo[6], Thierry Léonardis[4], Nadine Locoge[4], Nicolas Marchand[7], Stéphane Sauvage[4], Jean Sciare[8,9], Jean-François Doussin[1]

[1] LISA, Université de Paris, Université Paris-Est-Créteil, UMR CNRS 7583, Institut Pierre Simon Laplace (IPSL), Créteil, France

[2] Institut National de l'Environnement Industriel et des Risques, Verneuil-en-Halatte, France

[3] LaMP, CNRS UMR6016, Clermont Université, Université Blaise Pascal, Aubière, France

[4] IMT Lille Douai, Univ. Lille, SAGE - Département Sciences de l'Atmosphère et Génie de l'Environnement, 59000 Lille, France

[5] Laboratoire d'Aérologie, Université de Toulouse, CNRS, Toulouse, France

[6] Université Grenoble Alpes, CNRS, IRD, IGE, 38000 Grenoble, France

[7] Aix Marseille Univ, CNRS, LCE, Marseille, 13003, France

[8] LSCE, CNRS-CEA-UVSQ, IPSL, Université Paris-Saclay, Gif-sur-Yvette, France

[9] CARE-C, The Cyprus Institute, Nicosia, Cyprus

† deceased

Abstract

The characterization of the molecular composition of organic carbon in both gaseous and aerosol is key to understand the processes involved in the formation and aging of secondary organic aerosol. Therefore a technique using active sampling on cartridges and filters and derivatization followed by analysis using a Thermal Desorption-Gas Chromatography/mass spectrometer (TD-GC/MS) has been used. It aims at studying the molecular composition of organic carbon in both gaseous and aerosol phases during an intensive field campaign which took place in Corsica during the summer 2013: the ChArMEx (Chemistry and Aerosol Mediterranean Experiment) SOP1b (Special Observation Period 1B) campaign.

These measurements led to the identification of 51 oxygenated (carbonyl and or hydroxyl) compounds in the gaseous phase with concentrations comprised between 21 ng m^{-3} and 3900 ng m^{-3} and of 85

compounds in the particulate phase with concentrations comprised between 0.3 and 277 ng m^{-3}. Comparisons of these measurements with collocated data using other techniques have been conducted showing fair agreement in general for most species except for glyoxal in the gas phase and malonic, tartaric, malic and succinic acids in the particle phase with disagreements that can reach up to a factor of 8 and 20 on average, respectively for the latter two acids.

Comparison between the sum of all compounds identified by TD-GC/MS in particle phase with the total Organic Matter (OM) mass reveal that 18% of the total OM mass can be explained by the compounds measured by TD-GC/MS for the whole campaign. This number increase to 24% of the total Water Soluble OM (WSOM) measured by PILS-TOC if we consider only the sum of the soluble compounds measured by TD-GC/MS. This highlights the non-negligible fraction of the OM mass identified by these measurements but also the relative important fraction of OM mass remaining unidentified during the campaign and therefore the complexity of characterizing exhaustively the Organic Aerosol (OA) molecular chemical composition.

The fraction of OM measured by TD-GC/MS is largely dominated by di-carboxylic acids which represents 49% of the $PM_{2.5}$ content detected and quantified by this technique. Other contributions to $PM_{2.5}$ composition measured by TD-GC/MS are then represented by tri-carboxylic acids (15%), alcohols (13%), aldehydes (10%), di-hydroxy-carboxylic acids (5%), monocarboxylic acids and ketones (3% each) and hydroxyl-carboxylic acids (2%). These results highlight the importance of poly functionalized carboxylic acids for OM while the chemical processes responsible for their formation in both phases remain uncertain. While not measured by TD-GC/MS technique, HUmic-LIke Substances (HULIS) represent the most abundant identified species in the aerosol, contributing for 59% of the total identified OM mass on average during the campaign.

14 compounds were detected and quantified in both phases allowing the calculation of experimental partitioning coefficient for these species. The comparison of these experimental partitioning coefficients with theoretical ones, estimated by three different models, reveals large discrepancies varying from 2 to 7 orders of magnitude. These results suggest that the supposed instantaneous equilibrium being established between gaseous and particulate phases assuming a homogeneous non-viscous particle phase is questionable.

1 Introduction

It is now recognized that aerosols have an impact on human health, climate and ecosystems. However, large uncertainties still exist on their effects, especially on climate (Fiore et al., 2015). One of the key solution to reduce these uncertainties is to study the chemical composition of the aerosol organic

fraction since organic aerosols represent a large fraction of fine particles (Jimenez et al., 2009) which impacts are compound-dependent. Molecular characterization of organic aerosol is therefore crucial.

The OA fraction has been widely studied (e.g. De Gouw and Jimenez, 2009; Fuzzi et al., 2006; Glasius and Goldstein, 2016; Jacobson et al., 2000; Jimenez et al., 2009; Kanakidou et al., 2005; Pöschl, 2005; Robinson et al., 2007; Samake et al., 2019; Seinfeld and Pankow, 2003) and many studies allowed to improve our understanding of their molecular composition (e.g. Gallimore et al., 2017; Nguyen et al., 2013; Nozière et al., 2015; Zhang et al., 2011), their sources (e.g. Alves et al., 2012; Jiang et al., 2019; Shrivastava et al., 2007; Woody et al., 2016), and their formation and evolution processes (e.g. Chacon-Madrid and Donahue, 2011; Donahue et al., 2012; Heald et al., 2010; Li et al., 2016; Ng et al., 2011). Organic aerosol can be primary or secondary. Primary Organic Aerosols (POA) are directly emitted in the atmosphere, whereas Secondary Organic Aerosols (SOA) are formed after oxidation of gaseous organic precursors such as Volatile Organic Compounds (VOC). These gaseous compounds, coming from anthropogenic or natural sources, are progressively oxidized by atmospheric oxidants (OH, O_3 and NO_3). During this multigenerational oxidation process, the O/C ratio of the product formed rises and their volatility decreases allowing them to condense on existing particles or to form new particles through nucleation processes (Kulmala et al. 2013), leading to SOA formation. Some of the Semi-Volatile Organic Compounds (SVOC) formed during the process can be split between the particulate and gaseous phases. Hamilton et al. (2004) have studied the chemical composition of $PM_{2.5}$ collected in the urban atmosphere of London using a TD-GCxGC-ToF/MS (Thermal desorption comprehensive two dimensional-Gas Chromatography-Time of Flight mass Spectrometer) instrument highlighting the presence of more than 10 000 different organic compounds. In the same study, 130 Oxygenated Volatile Organic Compounds (OVOC) were also identified while the total number of different VOC in the atmosphere is estimated to be between 10 000 and 100 000 (Goldstein and Galbally, 2007). The large number of species composing the gaseous and particulate phases makes an exhaustive characterization of the atmospheric organic matter challenging.

For this reason, analysis of principal component is often used to describe aerosol composition. Among them, Positive Matrix Factorization (PMF) applied to Aerosol Mass Spectrometer (AMS) spectra allows retrieving more information on the sources and nature of organic aerosol. Although this classification allows getting insight into the oxidation state of OA, it is not possible to identify chemical processes involved in SOA formation and aging.

It is therefore essential to perform molecular characterization of organic aerosol. Several techniques allow this molecular characterization of OA, for example making use of off-line analyses of filter samplings or online analysis following direct sampling. Coupling Particle Into Liquid Sampler (PILS) to ion chromatography allow for example the measurement of organic species such as acetate, formate,

oxalate and methane sulfonic acid (MSA) (Orsini et al., 2003; Sciare et al., 2011). Parshintsev et al. (2009) also coupled PILS with gas chromatography mass spectrometry (GC-MS), which allowed the measurement of species such as alpha-pinene, pinonaldehyde, cis-pinonic and pinic acids. More recently, PILS was coupled to ultra-high performance liquid chromatography and electrospray ionization – quadrupole – time of flight – mass spectrometry (UPLC/ESI-Q-TOF-MS) allowing the measurement of species as diverse as adenine, adonitol, sorbitol, adipic acid, vanillic acid, azelaic acid cis-pinonic acid and palmitic acid (Zhang et al., 2016). Several studies also use tandem mass spectrometry (MS/MS or MS^n) to get some structural information on compounds present in the organic aerosol thanks to multiple fragmentation (e.g. Fujiwara et al., 2014; Kitanovski et al., 2011; Liu et al., 2015; Nguyen et al., 2011). This technique has led to the identification of species such as carboxylic acids, polycyclic aromatic hydrocarbons (PAH), oxy and nitro-PAH but also oligomers from isoprene photo-oxidation experiments in the presence of low or high NOx concentrations. Development of two-dimensional chromatography (GCxGC or LCxLC) allows reaching lower detection limit separation capacity and allows measuring a larger range of compounds (Hamilton et al., 2004; Parshintsev and Hyötyläinen, 2015). Online chromatographic systems also exist to analyze the composition of the particulate phase. However, difficulties in particle sampling made this type of development challenging. Williams et al. (2006) developed a thermo-desorption Aerosol GC/MS-Flame Ionization Detector (FID) allowing the online measurement of compounds of low polarity and with a small number of chemical functions. GC analysis is usually restricted to compounds of low polarity which excludes a lot of secondary component of OA. A derivatization step is therefore often used before the analysis or even during the sampling to perform OA chemical characterization. For example, O-(2,3,4,5,6-PentaFluoroBenzyl)HydroxylAmine (PFBHA) can be used for measurements of carbonyl compounds, and N,O-bis(trimethylsylil)-trifluoroacetamide (BSTFA) is used to reduce the polarity of hydroxyl compounds (Chiappini et al., 2006; Flores and Doskey, 2015; Pietrogrande et al., 2009; Schoene et al., 1994).

In addition of sample preparation and detection system, different types of extraction systems exist to avoid multiple steps prior to analysis. For example, Chiappini et al. (2006) have developed a technique using Supercritical Fluid Extraction (SFE)-GC/MS. With this technique, compounds are extracted from the filter by supercritical CO_2 including a derivatization step with BSTFA as reagent inside the extraction cell. Extraction efficiency depends on compound solubilities in the supercritical CO_2 which has a very high solvatation power. Thermo-desorption (TD) is another technique allowing to free from preparation steps prior to analysis. This technique relies on the volatilization of collected compounds and is suitable for semi-volatile constituent of SOA. It has the advantage to be commercially available with fully automatized systems, high sensibility allowing the analysis of very low quantity of aerosol

and low preparation time requirement limiting the risk of loss or contamination of analyzed samples (Hays and Lavrich, 2007; Parshintsev and Hyötyläinen, 2015). This technique has been used by Bates et al. (2008) and van Drooge et al. (2009) to quantify particulate PAH, while Ding et al. (2009) used it to measure PAH, alkanes, hopanes and steranes in $PM_{2.5}$.

Although numerous analytical methods exist for SOA chemical characterization, the multiphasic state of lots of compounds is rarely studied. Indeed, gaseous phase chemical characterization is often studied separately using techniques such as Proton Transfer Reaction (PTR)/MS (Hansel et al., 1995; de Gouw and Warneke, 2007; Holzinger et al., 2019) or online/offline GC techniques coupled to various detectors (e.g. FID, MS) (e.g. Barreira et al., 2015; Kajos et al., 2015; Valach et al., 2014). Despite this disconnected treatment between aerosol and gaseous phases, understanding mechanisms controlling the partitioning of SVOC between both phases is key to understand the formation and fate of SOA. A partition coefficient is defined according to the thermodynamic equilibrium to calculate the mass transfer of SVOC into particulate phase (Pankow, 1994). This equilibrium is thought to be dominated by absorption phenomena (Liang et al., 1997) and partition coefficient is therefore calculated accordingly in models. However, the validity of the instantaneous equilibrium between both phases as well as the predominance of absorption processes in the mass transfer process are questionable (Bateman et al., 2015; Fridlind et al., 2000; Healy et al., 2008; Rossignol et al., 2012; Virtanen et al., 2010). It is therefore crucial to test the theoretical partition coefficient against values measured in the field for which in situ measurements of organic compounds in both phases are needed.

The Mediterranean Basin is an excellent location to study organic aerosol formation and aging since it experiences intensive natural and anthropogenic emissions as well as strong photochemistry (Lelieveld et al., 2002). The ChArMEx project (Chemistry and Aerosols Mediterranean Experiments) aimed at assessing the present and future state of the atmosphere in the Mediterranean basin. In this frame, an intensive field campaign was performed at Cape Corsica for 3 weeks during summer 2013 setting up numerous instruments to investigate the chemical composition of aerosol and gaseous phases.

As part of this project, this study aims at characterizing the molecular composition of organic carbon in both the gaseous and aerosol phases during the campaign using TD-GC/MS measurements. These measurements were first compared to measurements performed with other techniques (offline cartridges analysis using HPLC and GC/FID-MS as well as PTR-MS for gaseous measurements and filter analysis using Ion chromatography, GC/MS and HPLC). These measurements were used to assess the composition of organic carbon and to estimate the experimental partition coefficient of compounds measured in both phases to be compared with theoretical values.

2 The ChArMEx field campaign

2.1 Description of the Cape Corse ground site

The ChArMEx field campaign took place from July 15th to August 5th 2013 at Ersa in Cape Corsica (42.97°N, 9.38°E) at the top of a hill (533 meters above sea level). The site is located at the northern tip of a thin peninsula, a few kilometers from the sea in all directions (between 2.5 and 6 km) and approximately 30 km north from the nearest urban area (Bastia). Mountains (peaking between 1000 and 1500 m) are limiting transport of urban air masses to the sampling site. The site is surrounded by typical vegetation of Mediterranean areas (maquis shrubland). Apart from this local biogenic influence, the site is mainly influenced by marine, and other natural (e.g. dust) emissions, and by continental and aged air masses due to long range transport. During summer, recirculation of air masses favors secondary aerosol and ozone build up (Millan et al., 1997). More details about the site, atmospheric conditions encountered during the campaign and air mass origin can be found in Michoud et al. (2017).

2.2 Sampling devices and TD-GC/MS analysis for the molecular characterization of multiphase organic carbon

Simultaneous sampling of gas and particulate phases has been conducted using a parallel sampling system with two independent pumps allowing the selection of flow rates specifically adjusted for each phase

Following the sampling, the molecular characterization of gaseous and particulate oxygenated organic compounds sampled during the campaign has been made using a TD-GC/MS analysis after derivatization steps following the method developed by Rossignol et al. (2012).

2.2.1 Gaseous phase

2.2.1.1 Gaseous phase sampling

Sampling of gaseous oxygenated compounds was achieved by using commercial sorbent cartridges containing Tenax TA (porous polymers based on 2.6-diphenyl-p-phenylene oxide; Perkin Elmer™ or Markes™) that has been previously impregnated with suitable derivatization agents (see below) following an improved protocol from Rossignol et al. (2012). To maximize the adsorption surface, small particle size of 60/80 mesh has been selected. Ambient air samplings were performed during 6h at a flow rate of 100 mL min^{-1}. A Teflon filter (Zefluor™ membrane, Pallflex™, 47 mm) was installed upstream from the cartridges to trap particulate compound that could potentially be adsorbed on Tenax adsorbent. Gaseous phase sampling has been performed using individual pumps (Gilian™ pump, model LFS-113DC). Prior to sampling, cartridges were heated at 320°C under a small helium flow rate during 4h to eliminate any trace of contamination. Every single cartridge was then analyzed to ensure

its cleanliness with quantities below Limit of Detection (LOD) for all measured compounds. During the campaign, 177 gaseous samples were collected following this protocol.

2.2.1.2 Sample preparation for gaseous phase

For the analysis of multi-functionalized OVOC by gas chromatography, a derivatization step is needed. It allows the suppression of the reactivity of functions, improving their thermal stability and rising their volatility. The dual derivatization reagents used in this study are PFBHA for carbonyl compounds and MTBSTFA (N-tert-Butyldimethylsilyl-N-methyltrifluoroacetamide) for hydroxyl compounds. The two derivatization processes are performed separately.

2.2.1.2.1 Carbonyl compounds

PFBHA has been used as derivatization reagent for the analysis of carbonyls. Cartridges have been impregnated prior to sampling thanks to a glass balloon with 8 arms, containing 0.33mg of solid PFBHA per cartridges mounted on the balloon, and on which the cartridges are installed under a 100 mL min^{-1} nitrogen flow rate per cartridges at 110°C during 20 minutes. The impregnated cartridges are stored at room temperature until the sampling. After sampling, cartridges are stored at room temperature during 5 days, optimum for the derivatization step using PFBHA (Ho and Yu, 2002), before their analysis.

2.2.1.2.2 Hydroxyl compounds and carboxylic acids

MTBSTFA with 1% of TBDMCS (tert-butyldimethylchlorosilane, used as catalyst for the reaction) has been used as derivatization agent for the analysis of hydroxyl compounds. Cartridges are impregnated prior to sampling vaporizing 0.3 µL of MTBSTFA at 275°C using a commercial thermal tube desorber (Dynatherm Analytical Instruments, model 890) under a flow of Helium of 30 mL min^{-1} for 11 minutes. The cartridges are then stored at room temperature and sampling is performed within 10 days after impregnation. After sampling, cartridges are stored at 4°C. To ensure complete derivatization of all compounds before the analysis, two deposits of 0.3 µL of MTBSTFA are achieved on each side of the cartridges which are kept at 60°C during 5h after that. Once the cartridges are back at room temperature, analysis is performed within 5 hours.

2.2.2 Particulate phase

2.2.2.1 Particulate phase sampling

Sampling of particulate matter was performed over regular (not impregnated) filters and derivatization was performed only after sampling (to avoid chemisorption of gaseous compounds on filters) following a protocol adapted from Rossignol et al. (2012). The sampling device used during the campaign was a modified Speciation Sampler Partisol, model 2300 (Rupprecht & Patashnick Co, Thermo Fisher Scientific). Three ChemComb cartridges, with $PM_{2.5}$ impactors, were mounted to this device to allow

the sampling of particulate phase on filters of different nature according to targeted compounds. For carbonyls compounds and non-oxygenated compounds Quartz filters (Pallflex™, 47 mm) were used. For hydroxyl compounds, quartz filters are not suitable because of silanol groups present at their surfaces that can be derivatized instead of the hydroxyl compounds reducing considerably their derivatization yield (Rossignol, 2012). Therefore, for the sampling of this type of compounds, we selected filters of borosilicate glass fibers coated with tetrafluoroethylene (TFE) called hereafter "Teflon quartz filters" (Fiber film, Pallflex™, 47mm). Activated carbon honeycomb denuders were installed upstream from the filters to avoid positive artifacts due to adsorption of gaseous oxygenated compounds on the filters. For cleaning and a best efficiency, denuders were heated at 250°C before being used for each new sample. The sampling flow rate was of 1 m^3 h^{-1} for each sample step. Quartz and Teflon quartz filters were carbonized prior to the sampling respectively at 500°C and 300°C to eliminate any possible contamination. During the campaign, 240 particulate samples were collected following this protocol.

2.2.2.2 Sample preparation for particulate phase

2.2.2.2.1 Carbonyl compounds

Sampling are performed on quartz filters which are stored at -16°C after sampling waiting for analysis. Then, the filters are cut into two pieces, both inserted into empty and clean stainless steel tubes. These tubes, including grids, are previously sonicated in several bath of ultra-pure water and acetonitrile and then are heated at 400°C under a flow of helium (80mL min^{-1}) during 4h. Deposition of 50 µL of PFBHA saturated solution (acetonitrile/water (90/10, v/v) with 27 mg mL^{-1} of PFBHA) are achieved in the tubes to expose adsorbed compounds to the derivatization reagent. Tubes are then stored at room temperature during 5 days to allow derivatization of adsorbed compounds before their analysis.

2.2.2.2.2 Hydroxyl compounds and carboxylic acids

Sampling are performed on Teflon quartz filters which are stored at -16°C after sampling waiting for analysis. Derivatization is performed after sampling directly on filters. Filters are put in stainless steel tubes cleaned following the same protocol than for carbonyl compounds. Tubes are then sealed and maintained vertically with 10 µl of MTBSTFA put in the bottom cap for passive impregnation during 24h at room temperature.

2.3.3 Analytical system

The analytical system used in this study is composed by three successive modules: a thermal desorption system, a gas chromatography unit and a mass spectrometer.

The thermal desorption allows the extraction of adsorbed compounds on sample support by increasing the temperature without any preliminary solvent extraction and collecting them on a cold trap before

flash injection in GC/MS instrument. The thermal desorption system (Markes™, model unity 1) is coupled with an automated system (Markes™, model Ultra 50:50). Thermal desorption parameters are listed in Table 1.

The GC/ MS instrument (Agilent Technologies Inc.) used during this study is composed by two modules:

- A GC unit, model 6890 A, associated with a capillary column Integra-Guard Rxi®-5Sil MS (stationary phase: 1.4-bis(dimethylsiloxy)phenylene dimethyl polysiloxane, length: 60m, diameter: 0.25mm, film thickness: 0.25µm, with 5m pre-column deactivated without any stationary phase; Restek Corporation).
- A Mass spectrometer, model 5973N, equipped with an ionization source in EI (Electronic Impact) or CI (Chemical Ionization; using CH_4 as reagent gas) and associated with a quadrupole.

GC/MS parameters are listed in Table 1.

2.3.4 Internal calibration protocol

For a more efficient quantification, internal calibration has been set up for both family of compounds (carbonyl and hydroxyl) and for both phases. This procedure aims at taking into account drift in MS sensitivity and derivatization efficiency. Two types of internal standards are used: substitutes which are deuterated compounds getting at least one derivatized function; and an internal standard which is a compound with no derivatized function. 50 ng of Substitutes are added prior to the derivatization step to take into account every steps of sample preparation as well as analysis steps. The list of substitutes selected is given in Table 2. The internal standard selected is pentadecane, because of its low volatility which limit signal variability due to evaporation of the internal standard before the analysis, and 50 ng is added on cartridges grid just before the analysis.

2.3.5 Estimation of uncertainties

Overall uncertainties have been determined taking into account precision, detection limit and systematic errors (including uncertainties on standard concentrations, on calibration, on blank determination and on sampling volume; following Gaussian error propagation). Overall uncertainties have therefore been estimated to be 35% and 54% on averaged in gas phase for carbonyls and hydroxyls and carboxylic acids respectively and to be 41% and 47% on averaged in particulate phase for carbonyls and hydroxyls and carboxylic acids respectively.

2.4 Ancillary measurements

An important set of complementary instruments, dedicated to the measurement of both gaseous and particulate phase, has been deployed at the supersite supporting the interpretation and validation of the TD-GC/MS dataset.

2.4.1 Gaseous ancillary measurements

2.4.1.1 PTR-MS

Measurements of OVOCs (e.g. nopinone, sum of methacrolein and methyl vinyl ketone, propanoic acid and methyl ethyl ketone), among other species (e.g. aromatics and biogenic VOCs) were performed using a Proton Transfer Reaction-Time of Flight Mass Spectrometer (PTR-ToF-MS, KORE Inc® 2nd generation). A detailed description of these measurements was given by Michoud et al. (2017, 2018). Briefly, ambient air was sampled through a 5-m long Teflon PFA (PerFluroAlkoxy) line held at 50°C at a flow rate of 1.2 L min^{-1}, leading to a residence time of 3.1s in the sampling line. The PTR-ToF-MS sampling flow rate was set at 150 mL min^{-1}. The instrument was operated at a reactor pressure and a temperature of 1.33 mbar and 40°C, respectively, leading to an E/N ratio of 135 Td.

An automated zero procedure was performed every hour for 10 min. Humid zero air was generated by passing ambient air through a catalytic converter to perform zeros at the same relative humidity than ambient air.

Signals from protonated VOCs were normalized by the signals of H_3O^+ and the first water cluster $H_3O^+(H_2O)$ as proposed by de Gouw and Warneke (2007). Concentrations were calculated using Eq. (1):

$$[R] = \frac{i_{R\_net}}{(i_{H_3O^+} + X_r . i_{H_3O^+(H_2O)})} . \frac{150000}{R_{f,R}} \quad (1)$$

Where [R] represents the mixing ratio of a given VOC, i_{R_net} the net signal of this VOC, i_{H3O+} and $i_{H3O+(H2O)}$ the signals of H_3O^+ and $H_3O^+(H_2O)$ at m/z 19 and 37 respectively recorded at m/z 21 and 39 to avoid any saturation of the detector and recalculated using the isotopic ratio between ^{16}O and ^{18}O. Xr is a factor introduced to account for the effect of humidity on the PTR-MS sensitivity (de Gouw and Warneke, 2007) and is determined experimentally through calibrations performed at various relative humidity. $R_{f,R}$ is the sensitivity determined during calibration experiments (in ncts ppt^{-1}) and normalized to 150 000 counts s^{-1} of H_3O^+ ions. The latter is the number of counts of reagent ions (not corrected for ion transmission into the ToFMS) observed on this PTR-ToF-MS instrument. Data were recorded at a time resolution of 1 min. During the campaign, calibrations were performed every 3 days using various standards, including a canister containing 15 VOCs (NMHCs, OVOCs and chlorinated VOCs; Restek®), a gas cylinder containing 9 NMHCs (Praxair®) and a gas cylinder containing 9 OVOCs (Praxair®). Information about the composition of these standards can be found in Michoud et al. (2017). Overall uncertainties are estimated between 6 and 23% depending on the compound considered (Michoud et al., 2017) following the "Aerosols, Clouds, and Trace gases Research InfraStructure network" (ACTRIS) guidelines for uncertainty evaluation (ACTRIS, 2012).

2.4.1.2 GC-FID/MS

OVOCs, including aldehydes, ketones, alcohols, ethers, esters, as well as a few NMHCs, including BVOCs and aromatics, were measured using an online GC/FID-MS instrument. This instrument as well as its setup during the campaign was described by Michoud et al. (2017). Briefly, ambient air was sampled via a KI ozone scrubber and a 5-m long PFA line (1/8") at a flow rate of 15 mL min^{-1} using an Air server-unity I (Markes International®). The sample was pre-diluted (50% dilution) with dry zero air to keep relative humidity below 50%. The sample was then collected in an internal trap, consisting in a 1.9 mm i.d. quartz tube filled with two different sorbents (5 mg of Carbopack B and 75 mg of Carbopack X, Supelco®) and cooled at 12.5 °C by a Peltier system. Compounds trapped on the sorbents were then thermally desorbed at 280 °C and injected into the column of a GC (Agilent®) equipped with a FID for detection and quantification and with a Mass Spectrometer (MS) for identification. The compounds were separated through a high polar CP-lowox column (30 m×0.53 mm× 10 µm) (Varian®). The time resolution of these measurements is 1h30min. Calibrations were performed during the campaign using a gas cylinder containing 29 VOCs (Praxair). Information about the composition of this standard can be found in Michoud et al. (2017). Overall uncertainties are estimated between 5 and 14% depending on the compound considered (Michoud et al., 2017) following ACTRIS guidelines for uncertainty evaluation (ACTRIS, 2012).

2.4.1.3 Active sampling on DNPH cartridges

Carbonyl compounds were collected continuously for 3 h durations by active sampling on DNPH cartridges (Waters®) using an automatic sampler (Tera Environment®). Cartridges were then eluted with 3 mL of acetonitrile to extract these compounds; and an aliquot of 20µL was analyzed later by High Performance Liquid Chromatography (HPLC) with UV detection. Ambient air was sampled via a 3-m PFA line (1/4") at 1.5 L min^{-1} and passed through a KI ozone scrubber and a stainless-steel particle filter (porosity: 2µm). More details about these measurements are given by Michoud et al. (2017; 2018). Calibrations were performed at the laboratory using Supelco® standard for DNPH. Overall uncertainties are estimated around 25% (Michoud et al., 2017) following ACTRIS guidelines for uncertainty evaluation (ACTRIS, 2012).

2.4.1.4 Inorganic trace gases

During the campaign, NO and NO_2 were measured by a commercial ozone chemiluminescence analyzer (Cranox II; Eco Physics®) with a time resolution of 5 min. NO was measured directly, while NO_2 was converted into NO using a photolytic converter. O_3 was measured using a commercial analyzer (TEI 49i; Thermo Environmental Instruments Inc®) using UV absorption with a time resolution of 5 min.

2.4.2 Particulate ancillary measurements

Mass concentrations of PM_{10} and PM_1 were measured during the campaign using two tapered element oscillating microbalance (TEOM) equipped with a filter dynamic measurement system (FDMS) (Thermo Scientific™). In addition, aerosol chemical composition was measured by online technique (aerosol chemical speciation monitor - ACSM) and offline-method (Ion chromatography, GC/MS and HPLC) on filters collected daily with 2 HiVol samplers (30 m^3 hr^{-1}) equipped with PM_1 and $PM_{2,5}$ inlets.

2.4.2.2 ACSM

Measurements of the chemical composition of non-refractory submicron aerosol (NR-PM_1) have been carried out using a quadrupole ACSM (Aerodyne Research Inc., Billerica, MA, USA). These measurements have been described in detail by Michoud et al. (2017). Briefly, the calibration of this instrument with monodispersed (300 nm diameter) ammonium nitrate particles was performed 2 months before the campaign. Because ambient air was dried by a Nafion membrane and because ammonium nitrate was low during the campaign, constant collection efficiency (CE) of 0.5 has been kept. The Q-ACSM was operated continuously during the whole campaign at a time resolution of 30 min.

2.4.2.3 Ionic Chromatography (IC)

Soluble anions and cations were analyzed by ionic chromatography (IC, ThermoFisher ICS3000) following protocol similar to that described elsewhere (e.g. Jaffrezo et al., 1998). Briefly, 38 mm diameter sub-samples from each filter were soaked for 20 min in 10 mL of Milli-Q water with orbital shaking, and then filtered using 0,22 µm-porosity Acrodisc filters before analysis. ASA11-HC and CS16 columns were used for anions and cations analyses, respectively.

2.4.2.4 GC/MS

Organic markers were analyzed by gas chromatography (GC) coupled with mass spectrometry (MS) using the method developed by El Haddad et al. (2011). Filter samples were first spiked with 300µL of a solution containing the internal standard D6-Cholesterol ($C_{24}H_{40}D_{60}$). Accelerated Solvent Extraction (ASE Dionex 300) was performed with a mixture of acetone/dichloromethane (1/1 v/v) at 100bar and 100°C during 10 min. Sample extracts were concentrated using a Turbo Vap II under N_2 in a water-bath regulated at 40°C to a final volume of 500µL. A fraction of the extracts (50µL) was derivatized at 70°C for 90 min by adding 100µL of N,O-bis(triméthylsilyl)trifluoroacétamide (BSTFA containing 1% of TMCS). Derivatized extracts were then analyzed using a Thermo Trace Ultra GC coupled with a Polaris Q – ion trap operating in the electron impact mode. The GC was equipped with a TR-5MS capillary column (30 m × 0.25 mm i.d. × 0.25 µm film thickness). Aliquots of 1 µL were injected in split mode (split ratio 50) at 280°C. The column temperature program was held at 65°C hold for 2 min, and ramped at 6°C/min up to 300°C, followed by an isothermal hold at 300°C for 20 min. GC-MS response factors

were determined using authentic standards. Compounds, for which no authentic standard are available, were quantified using the response factor of compounds with analogous chemical structures. Field blank filters were also treated with the same procedure. Limit of quantification are comprised between 0.02 and 0.20 ng m^{-3} and overall uncertainties are estimated between 5 and 14% depending on the compound considered following LQ and uncertainty evaluation described by El Haddad (2011).

2.4.2.5 HPLC

The analysis of a large array of organic acids (including pinic and phthalic acids, and 3-MBTCA) was conducted using the same water extracts as for IC analyses. In brief, this was performed by HPLC-MS (GP40 Dionex with a LCQ-FLEET Thermos-Fisher ion trap), with negative mode electrospray ionization. The separation column is a Synergi 4 µm Fusion – RP 80A (250×3 mm ID, 4 µm particle size, from Phenomenex). An elution gradient was optimized for the separation of the compounds, with a binary solvent gradient consisting of 0.1% formic acid in acetonitrile (solvent A) and 0.1% aqueous formic acid (solvent B) in various proportions during the 40-minute analytical run (see supplementary material S1). Column temperature was maintained to 30 °C. Eluent flow rate was 0.5 ml min^{-1}, and injection volume was 250 µl. Calibrations were performed for each analytical batch with solutions of authentic standards. All standards and samples were spiked with internal standards (phthalic-3,4,5,6-d4 acid and succinic-2,2,3,3-d4 acid). The calculation of the final atmospheric concentrations was corrected with the concentrations of internal standards and of the procedural blanks, taking also into account the extraction efficiency varying between 76-116% (depending on the acid).

2.4.2.6 OCEC SUNSET field instrument

Concentrations of elemental carbon (EC) and organic carbon (OC) in $PM_{2.5}$ were obtained in the field from an OCEC Sunset field instrument (Sunset Laboratory, Forest Grove, OR, USA; Bae et al., 2004) operated at a flow rate of 8 L min^{-1} with a denuder set upstream to avoid adsorption of semi-volatile compounds on the filter collecting particles in the instrument. Data were obtained every 2 hours with this instrument.

2.4.2.7 PILS-TOC

PM_1 water-soluble organic compounds (WSOCs) were measured by a modified PILS (Brechtel Manufacturing Inc., USA; Sorooshian et al., 2006) coupled with an analyzer of total organic carbon (TOC; model Sievers 900; Ionics Ltd, USA). Sciare et al. (2011) and Michoud et al. (2017) described this technique and operating procedures used during the ChArMEx field campaign. Briefly, the PILS-TOC instrument was operated at a flow rate of 15 L min^{-1} with a dilution factor of 1.30. A 0.45 µm pore size diameter filter in polyethylene was set in-line in the aerosol liquid flow to analyze the water-soluble

OC fraction only and a VOC denuder was set upstream the collection to avoid semi-volatile VOC contamination. Daily blanks were conducted every day for 1h by placing a total filter upstream of the sampling system.

2.4.2.8 HULIS measurements

The water soluble HULIS fraction is analyzed according to a protocol described in detail in Baduel et al. (2009). Briefly, the water-soluble fractions obtained from aerosol samples are passed through a weak anion exchange resin (GE Healthcare®, HiTrap™ DEAE FF, 0.7cm ID x 2.5cm length) without any pre-treatment. After this concentration step, the organic matter adsorbed is washed with 12mL of a solution of NaOH 0.04M (J.T.Baker®, pro analysis) to remove neutral components, hydrophobic bases, inorganic anion, mono- and di-acids initially retained in the resin. Finally, $HULIS_{WS}$ are quickly eluted in a single broad peak using 4 mL of a high ionic strength solution of NaCl 1M (Normapur®). All flow rates are set at 1.0 mL min^{-1}. UV-Vis absorption spectra are measured on-line after the extraction system, using a diode array detector (Dionex UV-VIS 340U), and recorded in the range 220-550nm. The $HULIS_{WS}$ fraction is subsequently collected manually and the carbon content is analyzed with a DOC analyser (Shimadzu TOC-$V_{CPH/CPN}$) by catalytic burning at 680°C in oxygen followed by non-dispersive infrared detection of the evolved CO_2.

3 Results

3.1 Main conditions during the campaign

3.1.1 Meteorological conditions

Meteorological and environmental conditions are presented in Table 3. Relatively high temperatures were monitored during the campaign (up to 32°C) coinciding with high biogenic emissions from local vegetation and strong photochemistry (Michoud et al., 2017). These conditions led to high ozone concentrations during the campaign (65 pbbv on average for the overall sampling period and up to 111 ppbv for 5 min measurements), typical of this region during summer (e.g. Lelieveld, 2002; Di Biagio et al., 2015). High relative humidity was encountered at night with values reaching 100% coinciding with foggy conditions observed during several nights at the site. High wind speeds were monitored with maximum reached on the 30th of July 2013 (13.2 m s^{-1}). During the campaign, almost 40% of air masses came from the south-west sector and 20% from the western sector (see Figure 1). Winds coming from south-west sector are predominant during daytime and nighttime and correspond to wind speed maxima. Winds from the west and north-east are also recorded, but during daytime only. Low NO_x concentrations were observed during the campaign (0.57 ppbv on average) with a few spikes above 1 ppbv corresponding to local influence from traffic especially when air masses came from the south (e.g. 27th July).

3.1.2 Particles and organic fraction

Mean, median, maximum and minimum of mass concentrations of PM_{10}, PM_1 and organic fraction in NR-PM_1 are summarized in Table 3 for the whole campaign. The averaged mass concentrations for PM_{10} is 12.0 µg m^{-3}, comparable to observations performed at other remote sites located in the western Mediterranean basin (e.g. 15.5 µg m^{-3} at Montseny, Spain; 11.5 µg m^{-3} between 2010 and 2013 at Montsec, Spain; 14.6 µg m^{-3} at Monte Martano, Italy; 13 µg m^{-3} between 2010 and 2013 at Venaco, France – Moroni et al., 2015; Nicolas, 2013; Querol et al., 2009a, 2009b; Ripoll et al., 2015). The averaged mass concentrations for PM_1 was 8.3 µg m^{-3} during the campaign and represented an important fraction of PM_{10} (69% on average). The amount of PM_1 at Ersa is also comparable to what has been previously measured in other remote sites in the western Mediterranean basin (e.g. 8.2 µg m^{-3} at Montseny, Spain; 7.1 µg m^{-3} between 2010 and 2013 at Montsec, Spain – Minguillón et al., 2015; Ripoll et al., 2015). During the campaign, the organic fraction represented between 40 and 55% of PM_1 mass concentrations (mean of 3.7 µg m^{-3} representing 44% of PM_1 on average).

Time series of mass concentrations of PM_{10}, PM_1 and organic fraction in PM_1 are presented in Figure 2. Highest mass concentrations for PM_{10} and PM_1 are observed between 12 and 21 July (15.7 and 11.0 µg m^{-3} on average respectively for PM_{10} and PM_1). According to back trajectory analysis (Michoud et al., 2017) this period corresponds to low wind speed and hence stationary air masses. A decrease of PM_{10} concentrations is observed from 21 to 25 July (12.0 µg m^{-3} on average) while the ratio PM_1/PM_{10} and organic/PM_1 are the highest (comprised between 0.5 and 1 and 0.3 and 0.7 respectively). During this period, the PM_{10} and PM_1 fractions are almost the same. This period is characterized by higher wind speed and air masses coming from the north-eastern sector and therefore characterized by anthropogenic influence from northern Italy. From 26 to 29 July, a rise in PM_{10} mass concentrations is observed coinciding with the warmest temperature of the campaign and air masses coming from the south and characterized by biogenic influence (see Michoud et al., 2017). From 29 July to 3 August, PM_1 concentrations strongly decrease (from 9.3 to 2.6 µg m^{-3} on average) coinciding with higher wind speed and relative humidity while winds came from north-west and north-east directions (see Michoud et al. 2017). During the last period (3-5 August), increase of PM_{10} and PM_1 concentrations is observed and a clear diurnal cycle is monitored for both fractions corresponding to a raise in temperatures. Overall, the organic fraction evolution follows the one of the PM_1 mass fraction.

3.2 Results from the TD-GC/MS analysis

3.2.1 Compound identifications

Detection of functionalized compounds led to the identification of 23 carbonyl compounds and 28 hydroxyl compounds and carboxylic acids in the gaseous phase and of 30 carbonyl compounds and 55 hydroxyl compounds and carboxylic acids in the particulate phase. The entire list of these 97

compounds is presented in supplementary material 2 together with their retention time, their O/C ratio, their calculated saturation vapor pressure, the main fragments of their mass spectra, the method used for their identification, the substitute used to account for the derivatization efficiency, the external standard used for their quantification, the fragment used for quantification, the averaged concentrations measured in both phases, their limits of detection and quantification, and the averaged overall uncertainties. An example of chromatogram is also shown in supplementary material 3. For the carbonyl compounds, the mono-functionalized compounds identified contained from 3 (e.g. propanal) to 10 (e.g. decanal) carbon atoms and from 2 (e.g. glyoxal) to 5 (e.g. 4-oxopentanal) carbon atoms for the bi-functionalized compounds. For the hydroxyl compounds and the carboxylic acids, the mono-functionalized identified compounds contained from 3 (e.g. propanoic acid) to 18 (e.g. octadecanoic acid) carbon atoms. Several poly-functionalized compounds have also been identified: hydroxy-acids and di-acids from 2 (e.g. glycolic acid) to 8 (e.g. mandelic acid) carbon atoms; triols, di-hydroxy-acids, hydroxyl-di-acids, tri-acids from 3 (e.g. glycerol) to 9 (e.g. 2-Hydroxy-4-isopropyl-hexanedioic acid) carbon atoms; and two tetra-functionalized compounds (methyl-tetrols and citric acid).

It is worth noting that several compounds exhibited very close quantities in the air sample and in the blank (designed as "blank" in the supplementary material 2). Therefore, the presence of these compounds in the air sampled cannot be certain. For the compounds that have been quantified successfully and present concentrations significantly above the quantification limit (10σ above averaged blank measurements), higher levels are observed in the gas phase. The averaged concentrations ranged from 21 ng m^{-3} (Mandelic acid) to 1600 ng m^{-3} (glycerol) for hydroxyl compounds in the gas phase and from 0.3 (Pyruvic acid) to 277 (oxalic acid) ng m^{-3} in the particulate phase. For the carbonyl compounds, the averaged concentrations ranged from 85 ng m^{-3} (hexanone) to 3900 ng m^{-3} (4-Oxopentanal) in the gas phase and from 1 ng m^{-3} (e.g. methylpropanal or glyoxal) to 20 ng m^{-3} (4-methylpentanal) in the particulate phase. Figure 3 presents the distribution of all quantified compounds along their saturation vapor pressure and their O/C ratio. The phases in which these compounds were identified are also shown in Figure 3. While compounds only present in the gas or aerosol phase exhibit high and low saturation vapor pressure, respectively, some exceptions are noticeable. Indeed, some gaseous compounds have low vapor pressure (down to $10^{-8.6}$ atm) such as long chain linear mono carboxylic acids (up to 15 carbon atoms) and some compounds only found in the particle phase have high vapor pressure (up to $10^{-0.8}$ atm), normally incompatible with their presence in such phase, such as small mono carbonyls (e.g. methylpropanal, methylbutanone, 2-methylbutanal…). We also found compounds in both phases exhibiting high vapor pressure (up to $10^{-0.4}$ atm), which is normally incompatible with their presence in aerosol phase, such as small carbonyls (e.g. propanal, acrolein, methacrolein, MVK…). This latest point is discussed further in section 4.3.

3.2.2 Data intercomparison

A comparison of data measured by TD-GC/MS with other techniques available on site has been performed, for both phases, to test the reliability of these measurements.

3.2.2.1 Gas phase

Comparisons of TD-GC/MS data with PTR-ToF-MS and GC/FID/MS data averaged over the same sampling duration at a similar time step have been performed and are shown in Figure 4 and Figure 5. Fair agreement is found for nopinone (relative differences observed from 1% to 133%), the sum of methacrolein and methyl vinyl ketone (2-155%), propanoic acid (3-107%) and methyl ethyl ketone (0-140%) between TD-GC/MS measurements and measurements performed by PTR-ToF-MS. Good agreement is also found for methyl vinyl ketone (3-168%) and 2-hexanone (3-99%) between TD-GC/MS measurements and measurements performed by GC/FID/MS. Ranges of measured concentrations are similar between these techniques as well as the temporal variation.

Comparisons of TD-GC/MS measurements with DNPH cartridges analysis are presented in Figure 6. For these latter, only the first ten days of the campaign have been validated because of a leak issue in the sampling system of DNPH cartridges after that period (see Michoud et al., 2017). Ranges of concentrations are in the same order of magnitude between these two techniques for propanal (5-93%), acrolein (18-90%), methacrolein (8-83%), methyl ethyl ketone (17-87%), methylglyoxal (19-99%), hexanal (1-73%) and benzaldehyde (10-115%) even though it is difficult to conclude on their co-variation regarding the small number of data available and the low time resolution for these two techniques. However, glyoxal and methyl vinyl ketone present large differences between the two techniques (factor of 15 and 12 respectively). For glyoxal, Matsunaga (2004) recorded maximum concentrations of 154 ng m^{-3} (≈65 pptv) at a forested site at Moshiri in Hokkaido island, in summer. Washenfelder et al. (2011) recorded maximum glyoxal concentrations of 500 pptv at an urban site in Los Angeles in summer, while numerous glyoxal precursors exist in urban environment. Therefore, the concentrations measured by TD-GC/MS seem overestimated and measurements from DNPH cartridges analysis seem more consistent with these previous observations. Thermo-degradation of other heavier compounds adsorbed on the Tenax cartridges leading to glyoxal could be an hypothesis for this overestimation. In the case of methyl vinyl ketone, the good agreement observed between TD-GC/MS measurements and GC/FID/MS ones (see Figure 5) tends to indicate that the disagreement observed here is related to an underestimation of the concentrations measured by DNPH cartridge analysis. Furthermore, recent studies on humidity dependence of the DNPH–HPLC–UV method for some ketone compounds, revealed that the collection efficiency is inversely related to relative humidity, with up to 35 %–80 % of the ketones being lost for RH values higher than 50 % at 22 °C (Ho et al., 2014). Furthermore, dimerization issues for MVK during analyses using DNPH method has also

been identified, during more recent measurements, that can cause strong underestimation of this technique (>50%).

3.2.2.2 Particulate phase

Comparisons of results from filter analysis by TD-GC/MS and by Ion chromatography, GC/MS and HPLC have been performed and are shown in Figure 7 and Figure 8. The range of concentrations between TD-GC/MS analysis and other techniques are in the same order of magnitude for oxalic acid (relative differences observed from 1% to 111%), pinic acid (13-136%), 2-methylglyceric acid (15-87%), MBTCA (12-95%), glycolic acid (16-104%) and phtalic acid (3-90%). However, a discrepancy is found for malonic acid and tartaric acid which measurements differ both of a factor of 4 on averaged between TD-GC/MS and HPLC analyses. For methyl-tetrols, the analysis performed by TD-GC/MS did not allow to distinguish the two isomers. Temporal evolution of compounds shown in Figure 7 and Figure 8 are also similar from one technique to another, especially for oxalic acid and pinic acid.

Nevertheless, larger disagreements have been observed for some compounds (see Figure 8). An overestimation of TD-GC/MS analysis compared to HPLC analysis of a factor of 8 and 20 on average, respectively for malic acid ad succinic acid, is observed. For malic acid, the external standard used for the estimation of the response factor (glycolic acid) is maybe not appropriate which may explain this discrepancy. As a test, succinic acid and glutaric acid (two other di-acids) have been used as external standard for malic acid quantification with no improvement in the agreement observed. For succinic acid, the authentic standard has been used and such problem cannot explain the discrepancy observed. No interference in the peak region is observed and this cannot neither explain the differences observed.

On the whole, comparisons of TD-GC/MS with other techniques deployed during the campaign are satisfactory for both phases with results at least in the same order of magnitude for the measured absolute concentrations, except for some compounds. Therefore, these observations allow us to use TD-GC/MS data both in gas and aerosol phase to study further the behavior of organic carbon at a molecular level at cape Corsica during ChArMEx campaign, keeping however in mind the potential biases revealed during this data comparison exercise.

4 Discussions

4.1 Description of organic compounds behaviour during the campaign

Time series of every compounds measured by TD-GC/MS in both phases are presented in the supplementary material 4.

Concerning the gaseous phase, several linear mono-aldehydes (C_3 to C_{10}) have been detected and quantified in the same range of concentrations as what has been previously reported by the same

technique at another site in Corsica (Rossignol et al., 2016). These compounds are mainly primary compounds emitted by vegetation under stress conditions. For propanal and butanal, some chemical processes and anthropogenic primary sources (especially ship emission) can also be involved (Agrawal et al., 2008). During the campaign, these compounds in the gaseous phase are characterized by daily maxima during daytime and daily minima during nighttime, confirming the predominance of biogenic sources. This diurnal cycle is also found when these compounds are also measured in the particulate phase, which may indicate a thermodynamic equilibrium for these compounds between both phases. Their concentrations are higher at the end of the campaign (30th of July) coinciding with the warmest period suggesting higher local biogenic emission.

At the end of the campaign, an elevation of concentrations is also observed for nopinone, 4-oxopentanal, 2-propenoic acid, methacrylic acid, mandelic acid, glycolic acid and levulinic acid (see supplementary material 4), all known as oxidation products of biogenic compounds (e.g. Fruekilde et al., 1998; Matsunaga et al., 2004; Rossignol et al., 2012). During this period, air masses were coming from the southern sector and travelled during a short period of time (12 to 24h) above Corsica and Sardinia (Michoud et al., 2017; Zannoni et al., 2017). An increase of concentrations is also observed for some monocarboxylic acids such as propanoic acid, pentanoic acid, hexanoic acid, tridecanoic acid, tetradecanoic acid and pentadecanoic acid (see supplementary material 4). Several sources are possible for these compounds that can be either primary or secondary and either biogenic or anthropogenic, especially for small carboxylic acids (C_3 to C_6; Chebbi and Carlier, 1996). Longer chain carboxylic acids are often considered as primary compounds both from biogenic and anthropogenic sources. Nevertheless, the results we obtained here underline the ubiquitous nature of organic acids (including long chains) in the atmosphere. It is remarkable to observe that despite their widespread detection, the knowledge on their sources (including chemical processes) remain scarce. Ozonolysis of alkenes, reactions between aldehydes and HO_2, or hydrolysis of oligomers could be involved.

At the beginning of the campaign (from 13th to 15th July) we observed a rise in concentrations of 4-oxopentanal, 2-hexanone, glycolic acid, 2-propenoic acid and monocarboxylic acids from C_3 to C_7 ((see supplementary material 4). A spike of methacrolein is also observed the 13th of July, highlighting local emission of biogenic precursors as it is during the calm low wind cluster period (Michoud et al, 2017).

Concerning particulate compounds, observations are different than for that gaseous compounds. Indeed, an important peak of concentrations is observed for many compounds from 17th to 19th of July, e.g. 3-isopropylglutaric acid, 3-hydroxy-4,4-dimethylglutaric acid, ketonorlimonic acid, ketolimonic acid, tricarballylic acid and methyltartronic acid (see supplementary material 4). The four first compounds correspond to oxidation products of biogenic precursors such as pinenes and limonene. O/C ratios for these compounds are high, varying from 0.5 (3-isopropylglutaric acid) to 1.3

(methyltartronic acid). This period corresponds to a rise in aerosol mass concentration (see Figure 2), with stagnant air masses and very low wind speed (Michoud et al., 2017). Associated with strong photochemistry, this favored chemical processing and the formation of secondary products with high O/C ratio. Other compounds also show a rise in their concentrations at this time (see supplementary material 4): unsaturated carboxylic acids (crotonic acid, 2-hydroxy-3methyl-2-pentenoic acid), long-chain monocarboxylic acids (hexadecanoic acid and octadecanoic acid), dicarboxylic acids (malonic acid, succinic acid, glutaric acid), unsaturated dicarboxylic acids (maleic acid, fumaric acid, 3-methyl-2-pentendioic acid), erythrose (a triol compound), 2,3-dihydroxypropanoic acid (a dihydroxy acid), hydroxy-diacids (2-hydroglutaric acid, 2-hydroxy-4-isopropylhexandioic acid, 3-hydroxy-2-pentenedioic acid, 3-hydroxy-3-methylglutaric acid, 3-hydroxyhexandioic acid, malic acid) and also 2-MGA, 3-MBTCA and DHOPA.

Higher concentrations for DHOPA, 2-MGA, MBTCA, and HGA are observed from 20 to 24 July (see supplementary material 4). 2-MGA is formed, in presence of NO_x (Ding et al., 2014, Fu et al., 2009; Giorio et al., 2017), through the oxidation of methacrolein and methacrylic acid, both oxidation products of isoprene. This period is characterized by the highest NO_x concentrations of the campaign (averaged concentrations of 1 ppbv against 0.6 ppbv for the rest of the campaign). Some dicarboxylic acids (e.g. malonic acid, succinic acid and glutaric acid) also show a rise in their concentrations during this period. This suggest a strong photochemical activity with an important aging of the air masses collected and an advanced photochemical age for this period, also characterized by high OH missing reactivity observed at the site (Zannoni et al., 2017). On the contrary, from the 27th of July to the end of the campaign, levels of concentrations for these compounds decrease (see supplementary material 4) suggesting less aged air masses. This is also revealed by the higher (cis-pinonic acid + pinic acid)/MBTCA ratio observed during this last period (see supplementary material 4). Indeed, this ratio allows the evaluation of the oxidation state of air masses since cis-pinonic acid and pinic acid are first generation oxidation products of monoterpenes while MBTCA is known to be a higher generation oxidation product (Ding et al., 2014).

Observations of MSA (methanesulfonic acid, CH_3SO_3H) and water soluble HULIS are reported in supplementary material S5. MSA is an oxidation product of dimethyl sulfide (DMS), a gaseous compound emitted by marine phytoplankton activity, and is mostly present in particulate phase. MSA can therefore be used to identify influence of marine chemistry on aerosol composition. Higher MSA concentrations are observed on 23 to 28 July and on 4 August when air masses were coming from the west sectors and spent days above sea (see Michoud et al., 2017) and on the first period of the campaign (15-18 July) when air masses were stagnant with very low wind speed (see Michoud et al., 2017). In summer, HULIS are mostly formed through secondary oligomerization processes in the

particulate phase (Baduel et al., 2010). Higher water soluble HULIS concentrations are observed on 20-21 July when air masses are originating from north-east sector bringing continental aged air-masses (Michoud et al., 2017) and on 27 July when air masses were coming from the southern sector with large biogenic influence (Michoud et al. 2017). This is consistent with the formation of HULIS through secondary oligomerization processes in summer from both anthropogenic and biogenic precursors (Srivastava et al., 2018).

4.2 Molecular characterization of particulate matter

A time series of total mass quantified by TD-GC/MS in $PM_{2.5}$ is presented in Figure 9. This sum has been calculated using the QL/2 (quantification limit/2) value when data were below the limit of quantification. The sum of all the compounds measured by TD-GC/MS represents an average of 630 ng m^{-3} for the whole campaign with a minimum of 54 ng m^{-3} and a maximum of 2400 ng m^{-3} measured on the 17th of July.

This sum is also compared to the organic matter mass concentration in $PM_{2.5}$ (see Figure 9). OM is calculated using the organic carbon (OC) concentration measured by the SUNSET field instrument with a ratio between OC and OM of 1.9 for Cape Corsica as proposed by Michoud et al. (2017). On average 18% of the total OM mass can be explained by the compounds measured by TD-GC/MS for the whole campaign. From 12 to 29 July, oxygenated compounds measured by TD-GC/MS represent more than 20% on average of measured OM while they represented less than 10% between July 29 and August 4. If measured water soluble HULIS are added to these compounds, analysed compounds represent 36% of measured OM on averaged and up to 100% on 16 July.

Some of the compounds identified and quantified by TD-GC/MS, especially carboxylic acids, are soluble in aqueous phase. To allow a comparison between TD-GC/MS measurement and WSOC (Water Soluble Organic Carbon) measurements conducted by PILS-TOC, only soluble compounds measured by TD-GC/MS have been selected (see Figure 10). Indeed, we considered only the compounds having a Henry's law constant higher than 10^4 M atm^{-1}. For every compounds measured by TD-GC/MS, the Henry's law constants have been determined by the Structure Activity Relationship (SAR) developed by Raventos-Duran et al. (2010) using the online platform of GECKO-A model (Aumont et al., 2005; http://geckoa.lisa.u-pec.fr/generateur_form.php). At the end, 39 different compounds have been selected for the calculation of this sum and no aldehyde or ketone were kept in this selection.

Comparing the sums of compounds measured by TD-GC/MS considering only soluble ones or considering all of them reveals very similar behaviors and level of concentrations (see Figure 10). On average, soluble compounds represent 72% of the total concentration of PM measured by TD-GC/MS despite the important number of compounds not considered as soluble (26 compounds over 58 not

considered). Time series of soluble compounds measured by TD-GC/MS and of WSOM have similar behaviors with higher concentrations during the period comprised between 17 and 23 July and smaller concentrations at the end of the campaign. It is worth noting that WSOM corresponds to PM_1 while TD-GC/MS measurements concern $PM_{2.5}$. On average, the sum of the soluble compounds measured by TD-GC/MS represented 24% of the total WSOM measured by PILS-TOC. If measured water soluble HULIS are added to these soluble compounds, analysed water soluble compounds represent 58% of measured WSOM on averaged and up to 100% on 15 and 17 July.

Time series and average composition of the $PM_{2.5}$ measured by TD-GC/MS are presented respectively in Figure 11 and Figure 12. Almost half of the $PM_{2.5}$ measured by TD-GC/MS are characterized by di-carboxylic acid (49%) with oxalic acid being the most important by far. Other contributors to $PM_{2.5}$ composition measured by TD-GC/MS are tri-carboxylic acids (15%), alcohols (13%), aldehydes (10%), di-hydroxy-carboxylic acids (5%), monocarboxylic acids and ketones (3% each) and hydroxyl-carboxylic acids (2%). High concentrations of di-carboxylic acids are observed from 13 to 28 July (441 ng m^{-3} on average; 51% of the total OM measured by TD-GC/MS). After the 29th of July, the contribution of di-carboxylic acids decreases significantly to reach 30%. The end of the campaign is characterized by intense fresh local biogenic emissions leading to less processed air masses and OM composed mostly by mono-functionalized compounds. On a general basis, organic acids constitute the principal contributors to the fraction of organic aerosol measured by TD-GC/MS during this campaign while only few chemical processes are known to lead to their formation (see section 4.1). The identification of many di-carboxylic acids implies the existence of unknown chemical processes both in gaseous phase and even more probably in particulate phase to explain their formation (Hammes et al., 2019). These missing processes in chemical mechanism included in models might contribute to their inability to reproduce correctly the formation and aging of SOA. If HULIS are considered in this analysis, they represent 59% of the total identified OM mass on average, ranging from 21% of contribution at the beginning of the campaign to more than 80% at the end of the campaign (from 31 July to 3 August).

4.3 Partitioning of organic carbon between gaseous and particulate phases

Many of the compounds identified during the campaign are present in both the gas and aerosol phases. The partitioning coefficient is therefore key to understand processes governing the equilibrium between both phases. For the compounds present in both phases, an experimental partitioning coefficient can be determined following eq. 2 relying on the Pankow equilibrium.

$$K_{pe,i} = \frac{F_i / TSP}{A_i} \quad (2)$$

$K_{pe,i}$ corresponds to the experimental partitioning coefficient for the compounds i, F_i corresponds to the concentration in the particulate phase, A_i corresponds to the concentration in gaseous phase and

TSP (Total Suspended Particulate matter) corresponds to the total mass concentration of particles measured by TEOM-FDMS for PM_{10} (µg m^{-3}). Uncertainties for experimental partitioning coefficients take into account uncertainties on the measurement of concentrations in both phases (see section 2.3.5) and on the TEOM measurement (estimated to be 25%).

Further, another expression of the Pankow equilibrium allows for the determination of theoretical partitioning coefficients using eq. 3.

$$K_{pt,i} = \frac{760RTf_{om}}{MW_{om}\zeta_i 10^6 p^0_{L,i}} \quad (3)$$

$K_{pt,i}$ corresponds to the theoretical partitioning coefficient for the compounds I, R to the ideal gas constant, T to the temperature in Kelvin, f_{om} to the OM mass fraction, MW_{om} to the averaged molar mass of compounds constituting organic particulate matter(g mol^{-1}), ζ_i to the activity coefficient, $p^0_{L,i}$ to the saturation vapor pressure (Torr). Saturation vapor pressures have been determined at 295K (averaged temperature of the campaign) using three different models (Moller et al., 2008; Myrdal and Yalkowsky, 1997; Nannoolal et al., 2008). f_{om} has been set to 0.8 using the averaged OC/TC ratio measured by the SUNSET field instrument.

Experimental (averaged over the campaign) and theoretical partitioning coefficients obtained for compounds identified in both phases are presented in Table 4 and Figure 13 and are compared to experimental coefficient obtained in a previous field study in Corsica and a chamber study in the EUPHORE simulation chamber (Rossignol et al., 2016). For most of the compounds, experimental partitioning coefficients obtained for the three campaigns are relatively close to each other, with some differences that can however reach up to an order of magnitude (e.g. dimethylglyoxal or acrolein, even two orders of magnitude for glyoxal). These observed differences are small compared to the differences recorded between experimental and theoretical coefficients, with an observed underestimation of theoretical coefficients varying from 1 to 7 orders of magnitude. It is worth noting that the three models used for theoretical coefficients determination are in good agreement. Higher differences between experimental and theoretical coefficients are observed for hydroxyl compounds and carboxylic acids with a shift of the equilibrium toward the particulate phase for experimental partitioning coefficients. It is worth noting that a denuder is used upstream the filter collection to avoid overestimation of particulate organic matter due to adsorption of semi-volatile compounds onto the filter, therefore excluding potential positive artefact for concentrations of compounds in particulate phase that could have led to overestimation of experimental partitioning coefficients. Furthermore, underestimation of gaseous concentrations for these compounds in such high proportion is unlikely, especially when we look at the comparisons performed for OVOCs with other measurement

techniques (see section 3.2.2.1), even for compounds that shows strong disagreement between various analytical methods (e.g. glyoxal).

The differences observed between experimental and theoretical partitioning coefficient may be explained by the high humidity conditions encountered during the campaign (mean RH value of 70%, see Table 3). Indeed, theoretical partitioning coefficient as described by the Pankow equilibrium does not take into account the presence of an aqueous phase or a deliquescent aerosol, while, soluble organic compounds can split between gaseous, aqueous and particulate phase. Concerning the partitioning between the gaseous and aqueous phases, the Henry law's constant and the activity coefficients are considered to calculate the thermodynamic equilibrium.

These differences could also be explained by the fact that the equilibrium between both phases is not reached. This could be due to the viscosity of particles. Some studies showed that organic aerosol can be found in various states, from liquid to semi-solid (viscous) (Bateman et al., 2016; Booth et al., 2014, Shiraiwa et al., 2011; Virtanen et al., 2010). The viscosity of the particle can limit the diffusion inside the particle, which can lead to an inhomogeneity in the composition with the formation of a gradient of concentrations between the surface and the center of the particle (Chan et al., 2014; Davies and Wilson, 2015; Zobrist et al., 2011). The equilibrium could therefore only concern an external layer of the particle and the gaseous phase (Davies and Wilson, 2015); or on the contrary a semi-solid external layer, caused by the aging of the particle, could prevent the equilibrium to settle between the particulate bulk and the gaseous phase.

Furthermore, Soonsin et al. (2010) showed that the physical state of the particle can influence the activity coefficient of some compounds and especially of dicarboxylic acids. Partitioning coefficients are calculated considering a liquid phase for aerosols. Considering a solid or semi-solid phase for aerosols would lead to a decrease in the vapor pressure estimation for such compounds and therefore to higher theoretical partitioning coefficients.

In addition, polymerization and oligomerization processes in the particulate phase have been highlighted in previous studies through the identification of compounds with high masses (Hallquist et al., 2009; Kalberer et al., 2004; Lim et al., 2010; Tolocka et al., 2004). The formation of oligomers increases the viscosity of the particle during its aging (Abramson et al., 2013). These reactions could also explain the presence of semi-volatile compounds in the particulate phase in such high proportion, especially for carbonyls that have high vapor pressure and which should not be detected in the aerosol phase based on the theory. Indeed, numerous studies reveal the possibility of formation of oligomers, inside the particle, from carbonyls such as α-di-carbonyls, for example glyoxal or methylglyoxal (Gao et al., 2004a, 2004b; Hastings et al., 2005; Iinuma et al., 2004; Jang et al., 2002, 2003; Jang and Kamens,

2001; Liggio et al., 2005a, 2005b; Lim et al., 2010; Tolocka et al., 2004). These reactions are favored under low water content in the particles even though oligomer production from other reactions can also happen at high relative humidity and in the aqueous phase. On the contrary, under higher humidity conditions, oligomers can form back monomer compounds which in case of viscous particle can be trapped into the particulate phase. It is worth noting that higher experimental partitioning coefficients are found for most compounds on 20 July and 26-27 July while water soluble HULIS concentrations are at their maximum. HULIS are known to be formed through secondary oligomerization processes in summer (Baduel et al., 2010), supporting the hypothesis that these kind of processes might be partly responsible for the disagreement between experimental and theoretical partitioning coefficient.

Even if an analytical artifact cannot be ruled out, for example a fragmentation of oligomers to form back the monomer compounds during the analysis, numerous evidences support the experimental results presented here and suggest that the instantaneous equilibrium being established between gaseous and particulate phases assuming a homogeneous non-viscous particle phase is not fully representative of the real atmosphere.

Conclusion

A multiphasic molecular characterization of oxygenated compounds has been carried out during the ChArMEx SOP 1b field campaign held in Ersa Corsica during July 2013 using an analytical technique based on multi-support sampling (filters and adsorbent containing cartridges), derivatization procedure and TD-GC/MS analysis. The deployment of this analytical technique in the field allows the identification of 97 different compounds in the gas (24 different compounds) and aerosol (50 different compounds) phases, some of them being present in both phases (23 different compounds). These compounds include simple carbonyls, alcohols or carboxylic acids as well as multi-functional compounds up to four functional groups. Among all the quantified compounds, the important contribution of organic acids (67% of the organic aerosol concentration measured by TD-GC/MS) emphasizes the existence of unknown chemical processes both in the gaseous phase and even more probably in the particulate phase to explain their formation. The absence of such processes in chemical mechanisms may contribute to the inability of models to correctly reproduce the formation and aging of SOA.

Comparisons of these measurements with other measurements performed at the site when available reveal fair agreement on the whole for almost all compounds experiencing redundant measurement in both phase with concentrations at least in the same order of magnitude. Noticeable disagreements (larger than a factor of 8 and up to a factor of 15) have however been found for glyoxal in the gas phase

between TD-GC/MS measurements and DNPH cartridges analysis and for malic and succinic acid in the particulate phase between TD-GC/MS measurements and HPLC analysis. Nevertheless, comparisons of TD-GC/MS with other techniques deployed during the campaign are in general agreement, validating their use to conduct further analysis.

While the data obtained are very valuable to provide additional insight into the composition of organic matter for air masses encountered during the campaign, it is worth noting that it represents only a fraction of the total mass of organic matter. Indeed, an attempt to close the mass budget of organic aerosol using the TD-GC/MS measurements reveal that the sum of all particulate oxygenated organic compounds measured by this technique account for 18% of the total OM mass on average for the whole campaign. This portion of OM identified at the molecular scale is not constant and mostly depends on the oxidation state of the sampled air masses. If we only consider the soluble compounds measured by TD-GC/MS, they represent 24% of the total WSOM on average. Therefore, a sizeable fraction of the OM mass was identified by TD-GC/MS analysis, but a very large fraction of OM mass remained unidentified during the campaign, highlighting the complexity of an exhaustive characterization of the OA chemical composition at the molecular scale. An important fraction of this unidentified OM mass is due to HULIS.

Finally, for the compounds quantified in both the gas and the aerosol phases, a comparison between experimental and theoretical partitioning coefficients has been performed revealing in most cases a large underestimation by the theory reaching 1 to 7 orders of magnitude. It indicates that the partitioning theory is most often inappropriate, since it is based on the instantaneous equilibrium being established between gaseous and particulate phases, assuming a homogeneous non-viscous particle phase. Furthermore, the partitioning of semi-volatile compounds is influenced by meteorological conditions (humidity, temperature) and inherent properties of particles (viscosity, water content, organic fraction concentrations, acidity, etc.). In addition, the way these conditions impact the partitioning of semi-volatile compounds strongly depends on the physico-chemical properties of the considered compounds (solubility, saturation vapor pressure, reactivity, etc.).

Data availability.

Access to the data used for this publication is restricted to registered users following the data and publication policy of the ChArMEx program (http://mistrals.sedoo.fr/ChArMEx/ Data-Policy/ChArMEx_DataPolicy.pdf).

Author contributions.

VM and EH participated in the field campaign and prepared the paper with inputs from all co-authors. LC, ELG and JFD were involved in TD-GC/MS measurements and supervised this work. SD, IF, TL, NL and SS participated in the field campaign and were in charge of VOC measurements (GC-FID/MS, PTR-MS, Active sampling on DNPH cartridges). AC and FG were in charge of inorganic trace gases measurements (NOx and O_3). JS participated in the field campaign and was in charge of aerosol measurements by ACSM, OCEC instrument, PILS-TOC and IC. JLJ and NM were in charge of aerosol speciation measurements during the campaign through filter analysis (IC, GC/MS, HPLC, HULIS measurements).

Competing interests.

The authors declare that they have no conflict of interest.

Special issue statement.

This article is part of the special issue "CHemistry and AeRosols Mediterranean EXperiments (ChArMEx; ACP/AMT inter-journal SI)". It does not belong to a conference.

Acknowledgements.

This study received financial support from the MISTRALS and ChArMEx programs, ADEME, the French Environmental Ministry, and the Communauté Territoriale de Corse (CORSiCA project). This project was also supported by the CaPPA project (Chemical and Physical Properties of the Atmosphere), funded by the French National Research Agency (ANR) through the PIA (Programme d'Investissement d'Avenir) under contract ANR-11-LABX-0005- 01 and by the Regional Council Nord-Pas de Calais and the European Funds for Regional Economic Development (FEDER).

The authors also want to thank Eric Hamonou and François Dulac for logistical help during the campaign and all the participants of the ChArMEx SOP1b field campaign. This paper is dedicated to the memory of our friend and colleague Laura Chiappini, who passed away shortly after the campaign. Laura conceived the original idea for this work and created the conditions to have this experimental worked done. Analyses at IGE were performed on the Air O Sol plateform partly funded with the Labex OSUG@2020 (ANR10 LABX56)

References

Abramson, E., Imre, D., Beránek, J., Wilson, J. and Zelenyuk, A.: Experimental determination of chemical diffusion within secondary organic aerosol particles, Phys. Chem. Chem. Phys., 15(8), 2983–2991, doi:10.1039/C2CP44013J, 2013.

ACTRIS: Measurement Guideline VOC: WP4- NA4: Trace gases networking: Volatile organic carbon and nitrogen oxides Deliverable D4.1: Draft for standardized operating procedures (SOPs) for VOC measurements, 25–30, http://www.actris.net/Portals/97/deliverables/PU/WP4_D4.1_M12_v2.pdf (last access: 21 July 2020), 2012.

Agrawal, H., Welch, W. A., Miller, J. W. and Cocker, D. R.: Emission Measurements from a Crude Oil Tanker at Sea, Environ. Sci. Technol., 42(19), 7098–7103, doi:10.1021/es703102y, 2008.

Alves, C., Vicente, A., Pio, C., Kiss, G., Hoffer, A., Decesari, S., Prevôt, A. S. H., Minguillón, M. C., Querol, X., Hillamo, R., Spindler, G. and Swietlicki, E.: Organic compounds in aerosols from selected European sites – biogenic versus anthropogenic sources, Atmos. Environ., 59, 243–255, doi:10.1016/j.atmosenv.2012.06.013, 2012.

Aumont, B., Szopa, S. and Madronich, S.: Modelling the evolution of organic carbon during its gas-phase tropospheric oxidation: development of an explicit model based on a self generating approach, Atmos Chem Phys, 5(9), 2497–2517, doi:10.5194/acp-5-2497-2005, 2005.

Baduel, C., Voisin, D., and Jaffrezo, J. L.: Comparison of analytical methods for Humic Like Substances (HULIS) measurements in atmospheric particles, Atmos. Chem. Phys., 9, 5949–5962, https://doi.org/10.5194/acp-9-5949-2009, 2009.

Baduel, C., Voisin, D., and Jaffrezo, J.-L.: Seasonal variations of concentrations and optical properties of water soluble HULIS collected in urban environments, Atmos. Chem. Phys., 10, 4085–4095, https://doi.org/10.5194/acp-10-4085-2010, 2010.

Bae, M.-S., Schauer, J. J., DeMinter, J. T., Turner, J. R., Smith, D., and Cary, R. A.: Validation of a semi-continuous instrument for elemental carbon and organic carbon using a thermal-optical method, Atmos. Environ., 38, 2885–2893, 2004.

Barreira, L. M. F., Parshintsev, J., Kärkkäinen, N., Hartonen, K., Jussila, M., Kajos, M., Kulmala, M. and Riekkola, M.-L.: Field measurements of biogenic volatile organic compounds in the atmosphere by dynamic solid-phase microextraction and portable gas chromatography-mass spectrometry, Atmos. Environ., 115, 214–222, doi:10.1016/j.atmosenv.2015.05.064, 2015.

Bateman, A. P., Bertram, A. K. and Martin, S. T.: Hygroscopic influence on the semisolid-to-liquid transition of secondary organic materials, J. Phys. Chem. A, 119(19), 4386–4395, doi:10.1021/jp508521c, 2015.

Bateman, A. P., Gong, Z., Liu, P., Sato, B., Cirino, G., Zhang, Y., Artaxo, P., Bertram, A. K., Manzi, A. O., Rizzo, L. V., Souza, R. A. F., Zaveri, R. A. and Martin, S. T.: Sub-micrometre particulate matter is primarily in liquid form over Amazon rainforest, Nat. Geosci., 9(1), 34–37, doi:10.1038/ngeo2599, 2016.

Bates, M., Bruno, P., Caputi, M., Caselli, M., de Gennaro, G. and Tutino, M.: Analysis of polycyclic aromatic hydrocarbons (PAHs) in airborne particles by direct sample introduction thermal desorption GC/MS, Atmos. Environ., 42(24), 6144–6151, doi:10.1016/j.atmosenv.2008.03.050, 2008.

Booth, A. M., Murphy, B., Riipinen, I., Percival, C. J. and Topping, D. O.: Connecting bulk viscosity measurements to kinetic limitations on attaining equilibrium for a model aerosol composition, Environ. Sci. Technol., 48(16), 9298–9305, doi:10.1021/es501705c, 2014.

Chacon-Madrid, H. J. and Donahue, N. M.: Fragmentation vs. functionalization : chemical aging and organic aerosol formation, Atmospheric Chem. Phys., 11(20), 10553–10563, doi:10.5194/acp-11-10553-2011, 2011.

Chan, M. N., Zhang, H., Goldstein, A. H. and Wilson, K. R.: Role of Water and Phase in the Heterogeneous Oxidation of Solid and Aqueous Succinic Acid Aerosol by Hydroxyl Radicals, J. Phys. Chem. C, 118(50), 28978–28992, doi:10.1021/jp5012022, 2014.

Chebbi, A. and Carlier, P.: Carboxylic acids in the troposphere, occurrence, sources, and sinks: A review, Atmos. Environ., 30(24), 4233–4249, doi:10.1016/1352-2310(96)00102-1, 1996.

Chiappini, L., Perraudin, E., Durand-Jolibois, R. and Doussin, J. F.: Development of a supercritical fluid extraction–gas chromatography–mass spectrometry method for the identification of highly polar compounds in secondary organic aerosols formed from biogenic hydrocarbons in smog chamber experiments, Anal. Bioanal. Chem., 386(6), 1749–1759, doi:10.1007/s00216-006-0744-3, 2006.

Davies, J. F. and Wilson, K. R.: Nanoscale interfacial gradients formed by the reactive uptake of OH radicals onto viscous aerosol surfaces, Chem Sci, 6(12), 7020–7027, doi:10.1039/C5SC02326B, 2015.

De Gouw, J. and Jimenez, J. L.: Organic Aerosols in the Earth's Atmosphere, Environ. Sci. Technol., 43(20), 7614–7618, doi:10.1021/es9006004, 2009.

de Gouw, J. and Warneke, C.: Measurements of volatile organic compounds in the earth's atmosphere using proton-transferreaction mass spectrometry, Mass. Spectrom. Rev., 26, 223–257, doi:10.1002/mas.20119, 2007.

Di Biagio, C., Doppler, L., Gaimoz, C., Grand, N., Ancellet, G., Raut, J.-C., Beekmann, M., Borbon, A., Sartelet, K., Attié, J.-L., Ravetta, F. and Formenti, P.: Continental pollution in the western Mediterranean basin: vertical profiles of aerosol and trace gases measured over the sea during TRAQA 2012 and SAFMED 2013, Atmos Chem Phys, 15(16), 9611–9630, doi:10.5194/acp-15-9611-2015, 2015.

Ding, X., He, Q.-F., Shen, R.-Q., Yu, Q.-Q. and Wang, X.-M.: Spatial distributions of secondary organic aerosols from isoprene, monoterpenes, β-caryophyllene, and aromatics over China during summer, J. Geophys. Res. Atmospheres, 119(20), 2014JD021748, doi:10.1002/2014JD021748, 2014.

Donahue, N. M., Robinson, A. L., Trump, E. R., Riipinen, I. and Kroll, J. H.: Volatility and Aging of Atmospheric Organic Aerosol, in Atmospheric and Aerosol Chemistry, vol. 339, edited by V. F. McNeill and P. A. Ariya, pp. 97–143, Springer-Verlag Berlin, Berlin., 2012.

El Haddad, I. : Fractions primaire et secondaire de l'aérosol organique primaire et secondaire de l'aérosol organique primaire et secondaire de l'aérosol organique: Méthodologies et application à un environnement urbain méditerranéen, Marseille, Université de Provence. [online] Available from: https://tel.archives-ouvertes.fr/tel-00589732/document (Accessed 25 January 2021), 2011.

El Haddad, I., Marchand, N., Wortham, H., Piot, C., Besombes, J.-L., Cozic, J., Chauvel, C., Armengaud, A., Robin, D., and Jaffrezo, J.-L.: Primary sources of PM2.5 organic aerosol in an industrial Mediterranean city, Marseille, Atmos. Chem. Phys., 11, 2039–2058, https://doi.org/10.5194/acp-11-2039-2011, 2011.

Fiore, A. M., Naik, V. and Leibensperger, E. M.: Air Quality and Climate Connections, J. Air Waste Manag. Assoc., 65(6), 645–685, doi:10.1080/10962247.2015.1040526, 2015.

Flores, R. M. and Doskey, P. V.: Evaluation of multistep derivatization methods for identification and quantification of oxygenated species in organic aerosol, J. Chromatogr. A, 1418, 1–11, doi:10.1016/j.chroma.2015.09.041, 2015.

Fridlind, A. M., Jacobson, M. Z., Kerminen, V. M., Hillamo, R. E., Ricard, V., and Jaffrezo, J. L.: Analysis of gas-aerosol partitioning in the Arctic: Comparison of size-resolved equilibrium model results with field data, J. Geophys. Res., 105, 19 891– 19 903, 2000.

Fruekilde, P., Hjorth, J., Jensen, N. R., Kotzias, D. and Larsen, B.: Ozonolysis at vegetation surfaces : a source of acetone, 4-oxopentanal, 6-methyl-5-hepten-2-one, and geranyl acetone in the troposphere, Atmos. Environ., 32(11), 1893–1902, 1998.

Fu, P., Kawamura, K., Chen, J. and Barrie, L. A.: Isoprene, monoterpene, and sesquiterpene oxidation products in the high Arctic aerosols during late winter to early summer, Environ. Sci. Technol., 43(11), 4022–4028, doi:10.1021/es803669a, 2009.

Fujiwara, F., Guiñez, M., Cerutti, S. and Smichowski, P.: UHPLC-(+)APCI-MS/MS determination of oxygenated and nitrated polycyclic aromatic hydrocarbons in airborne particulate matter and tree barks collected in Buenos Aires city, Microchem. J., 116, 118–124, doi:10.1016/j.microc.2014.04.004, 2014.

Fuzzi, S., Andreae, M. O., Huebert, B. J., Kulmala, M., Bond, T. C., Boy, M., Doherty, S. J., Guenther, A., Kanakidou, M., Kawamura, K. and others: Critical assessment of the current state of scientific knowledge, terminology, and research needs concerning the role of organic aerosols in the atmosphere, climate, and global change, Atmospheric Chem. Phys., 6(7), 2017–2038, 2006.

Gallimore, P. J., Giorio, C., Mahon, B. M., and Kalberer, M.: Online molecular characterisation of organic aerosols in an atmospheric chamber using extractive electrospray ionisation mass spectrometry, Atmos. Chem. Phys., 17, 14485–14500, https://doi.org/10.5194/acp-17-14485-2017, 2017.

Gao, S., Keywood, M., Ng, N. L., Surratt, J., Varutbangkul, V., Bahreini, R., Flagan, R. C. and Seinfeld, J. H.: Low-Molecular-Weight and Oligomeric Components in Secondary Organic Aerosol from the Ozonolysis of Cycloalkenes and α-Pinene, J. Phys. Chem. A, 108(46), 10147–10164, doi:10.1021/jp047466e, 2004a.

Gao, S., Ng, N. L., Keywood, M., Varutbangkul, V., Bahreini, R., Nenes, A., He, J., Yoo, K. Y., Beauchamp, J. L., Hodyss, R. P., Flagan, R. C. and Seinfeld, J. H.: Particle Phase Acidity and Oligomer Formation in Secondary Organic Aerosol, Environ. Sci. Technol., 38(24), 6582–6589, doi:10.1021/es049125k, 2004b.

Glasius, M. and Goldstein, A. H.: Recent discoveries and future challenges in atmospheric organic chemistry, Environ. Sci. Technol., doi:10.1021/acs.est.5b05105, 2016.

Goldstein, A. H. and Galbally, I. E.: Known and unexplored organic constituents in the earth's atmosphere, Environ. Sci. Technol., 41(5), 1514–1521, 2007.

Hallquist, M., Wenger, J. C., Baltensperger, U., Rudich, Y., Simpson, D., Claeys, M., Dommen, J., Donahue, N. M., George, C., Goldstein, A. H., Hamilton, J. F., Herrmann, H., Hoffmann, T., Iinuma, Y., Jang, M., Jenkin, M. E., Jimenez, J. L., Kiendler-Scharr, A., Maenhaut, W., McFiggans, G., Mentel, T. F.,

Monod, A., Prévôt, A. S. H., Seinfeld, J. H., Surratt, J. D., Szmigielski, R. and Wildt, J.: The formation, properties and impact of secondary organic aerosol: current and emerging issues, Atmos Chem Phys, 9(14), 5155–5236, doi:10.5194/acp-9-5155-2009, 2009.

Hamilton, J. F., Webb, P. J., Lewis, A. C., Hopkins, J. R., Smith, S. and Davy, P.: Partially oxidised organic components in urban aerosol using GCXGC-TOF/MS, Atmospheric Chem. Phys., 4(5), 1279–1290, 2004.

Hansel, A., Jordan, A., Holzinger, R., Prazeller, P., Vogel, W. and Lindinger, W.: Proton transfer reaction mass spectrometry: on-line trace gas analysis at the ppb level, Int. J. Mass Spectrom. Ion Process., 149–150, 609–619, doi:10.1016/0168-1176(95)04294-U, 1995.

Hastings, W. P., Koehler, C. A., Bailey, E. L. and De Haan, D. O.: Secondary Organic Aerosol Formation by Glyoxal Hydration and Oligomer Formation: Humidity Effects and Equilibrium Shifts during Analysis, Environ. Sci. Technol., 39(22), 8728–8735, doi:10.1021/es050446l, 2005.

Hammes, J., Lutz, A., Mentel, T., Faxon, C., and Hallquist, M.: Carboxylic acids from limonene oxidation by ozone and hydroxyl radicals: insights into mechanisms derived using a FIGAERO-CIMS, Atmos. Chem. Phys., 19, 13037–13052, https://doi.org/10.5194/acp-19-13037-2019, 2019.

Hays, M. D. and Lavrich, R. J.: Developments in direct thermal extraction gas chromatography-mass spectrometry of fine aerosols, TrAC Trends Anal. Chem., 26(2), 88–102, doi:10.1016/j.trac.2006.08.007, 2007.

Heald, C. L., Kroll, J. H., Jimenez, J. L., Docherty, K. S., DeCarlo, P. F., Aiken, A. C., Chen, Q., Martin, S. T., Farmer, D. K. and Artaxo, P.: A simplified description of the evolution of organic aerosol composition in the atmosphere: Van Krevelen Diagram of organic aerosol, Geophys. Res. Lett., 37(8), n/a–n/a, doi:10.1029/2010GL042737, 2010.

Healy, R. M., Wenger, J. C., Metzger, A., Duplissy, J., Kalberer, M. and Dommen, J.: Gas/particle partitioning of carbonyls in the photooxidation of isoprene and 1,3,5-trimethylbenzene, Atmos Chem Phys, 8(12), 3215–3230, doi:10.5194/acp-8-3215-2008, 2008.

Ho, S. S. H. and Yu, J. Z.: Feasibility of Collection and Analysis of Airborne Carbonyls by On-Sorbent Derivatization and Thermal Desorption, Anal. Chem., 74(6), 1232–1240, doi:10.1021/ac015708q, 2002.

Ho, S. S. H., Chow, J. C., Watson, J. G., Ip, H. S. S., Ho, K. F., Dai, W. T., and Cao, J.: Biases in ketone measurements using DNPHcoated solid sorbent cartridges, Anal. Methods-UK, 6, 967–974, https://doi.org/10.1039/C3AY41636D, 2014.

Holzinger, R., Acton, W. J. F., Bloss, W. J., Breitenlechner, M., Crilley, L. R., Dusanter, S., Gonin, M., Gros, V., Keutsch, F. N., Kiendler-Scharr, A., Kramer, L. J., Krechmer, J. E., Languille, B., Locoge, N., Lopez-Hilfiker, F., Materić, D., Moreno, S., Nemitz, E., Quéléver, L. L. J., Sarda Esteve, R., Sauvage, S., Schallhart, S., Sommariva, R., Tillmann, R., Wedel, S., Worton, D. R., Xu, K., and Zaytsev, A.: Validity and limitations of simple reaction kinetics to calculate concentrations of organic compounds from ion counts in PTR-MS, Atmos. Meas. Tech., 12, 6193–6208, https://doi.org/10.5194/amt-12-6193-2019, 2019.

Iinuma, Y., Böge, O., Gnauk, T. and Herrmann, H.: Aerosol-chamber study of the α-pinene/O3 reaction : influence of particle acidity on aerosol yields and products, Atmos. Environ., 38(5), 761–773, doi:10.1016/j.atmosenv.2003.10.015, 2004.

Jacobson, M. C., Hansson, H.-C., Noone, K. J. and Charlson, R. J.: Organic atmospheric aerosols: Review and state of the science, Rev. Geophys., 38(2), 267–294, doi:10.1029/1998RG000045, 2000.

Jaffrezo, J. L., Calas, N., and Bouchet, M.: Carboxylic acids measurements with ionic chromatography, Atmos. Environ., 32, 2705–2708, 1998.

Jang, M. and Kamens, R. M.: Atmospheric secondary aerosol formation by heterogeneous reactions of aldehydes in the presence of a sulfuric acid aerosol catalyst, Environ. Sci. Technol., 35(24), 4758–4766, doi:10.1021/es010790s, 2001.

Jang, M., Czoschke, N. M., Lee, S. and Kamens, R. M.: Heterogeneous Atmospheric Aerosol Production by Acid-Catalyzed Particle-Phase Reactions, Science, 298(5594), 814–817, doi:10.1126/science.1075798, 2002.

Jang, M., Carroll, B., Chandramouli, B. and Kamens, R. M.: Particle growth by acid-catalyzed heterogeneous reactions of organic carbonyls on preexisting aerosols, Environ. Sci. Technol., 37(17), 3828–3837, doi:10.1021/es021005u, 2003.

Jiang, J., Aksoyoglu, S., El-Haddad, I., Ciarelli, G., Denier van der Gon, H. A. C., Canonaco, F., Gilardoni, S., Paglione, M., Minguillón, M. C., Favez, O., Zhang, Y., Marchand, N., Hao, L., Virtanen, A., Florou, K., O'Dowd, C., Ovadnevaite, J., Baltensperger, U., and Prévôt, A. S. H.: Sources of organic aerosols in Europe: a modeling study using CAMx with modified volatility basis set scheme, Atmos. Chem. Phys., 19, 15247–15270, https://doi.org/10.5194/acp-19-15247-2019, 2019.

Jimenez, J. L., Jayne, J. T., Shi, Q., Kolb, C. E., Worsnop, D. R., Yourshaw, I., Seinfeld, J. H., Flagan, R. C., Zhang, X., Smith, K. A., Morris, J. W. and Davidovits, P.: Ambient aerosol sampling using the Aerodyne Aerosol Mass Spectrometer, J. Geophys. Res. Atmospheres, 108(D7), 8425, doi:10.1029/2001JD001213, 2003.

Jimenez, J. L., Canagaratna, M. R., Donahue, N. M., Prevot, A. S. H., Zhang, Q., Kroll, J. H., DeCarlo, P. F., Allan, J. D., Coe, H., Ng, N. L., Aiken, A. C., Docherty, K. S., Ulbrich, I. M., Grieshop, A. P., Robinson, A. L., Duplissy, J., Smith, J. D., Wilson, K. R., Lanz, V. A., Hueglin, C., Sun, Y. L., Tian, J., Laaksonen, A., Raatikainen, T., Rautiainen, J., Vaattovaara, P., Ehn, M., Kulmala, M., Tomlinson, J. M., Collins, D. R., Cubison, M. J., E., Dunlea, J., Huffman, J. A., Onasch, T. B., Alfarra, M. R., Williams, P. I., Bower, K., Kondo, Y., Schneider, J., Drewnick, F., Borrmann, S., Weimer, S., Demerjian, K., Salcedo, D., Cottrell, L., Griffin, R., Takami, A., Miyoshi, T., Hatakeyama, S., Shimono, A., Sun, J. Y., Zhang, Y. M., Dzepina, K., Kimmel, J. R., Sueper, D., Jayne, J. T., Herndon, S. C., Trimborn, A. M., Williams, L. R., Wood, E. C., Middlebrook, A. M., Kolb, C. E., Baltensperger, U. and Worsnop, D. R.: Evolution of Organic Aerosols in the Atmosphere, Science, 326(5959), 1525–1529, doi:10.1126/science.1180353, 2009.

Kajos, M. K., Rantala, P., Hill, M., Hellen, H., Aalto, J., Patokoski, J., Taipale, R., Hoerger, C. C., Reimann, S., Ruuskanen, T. M., Rinne, J. and Petaja, T.: Ambient measurements of aromatic and oxidized VOCs by PTR-MS and GC-MS: intercomparison between four instruments in a boreal forest in Finland, Atmospheric Meas. Tech., 8(10), 4453–4473, doi:10.5194/amt-8-4453-2015, 2015.

Kalberer, M., Paulsen, D., Sax, M., Steinbacher, M., Dommen, J., Prevot, A. S. H., Fisseha, R., Weingartner, E., Frankevich, V., Zenobi, R. and Baltensperger, U.: Identification of Polymers as Major Components of Atmospheric Organic Aerosols, Science, 303(5664), 1659–1662, doi:10.1126/science.1092185, 2004.

Kanakidou, M., Seinfeld, J. H., Pandis, S. N., Barnes, I., Dentener, F. J., Facchini, M. C., Van Dingenen, R., Ervens, B., Nenes, A., Nielsen, C. J., Swietlicki, E., Putaud, J. P., Balkanski, Y., Fuzzi, S., Horth, J.,

Moortgat, G. K., Winterhalter, R., Myhre, C. E. L., Tsigaridis, K., Vignati, E., Stephanou, E. G. and Wilson, J.: Organic aerosol and global climate modelling: a review, Atmos Chem Phys, 5(4), 1053–1123, doi:10.5194/acp-5-1053-2005, 2005.

Kitanovski, Z., Grgić, I. and Veber, M.: Characterization of carboxylic acids in atmospheric aerosols using hydrophilic interaction liquid chromatography tandem mass spectrometry, J. Chromatogr. A, 1218(28), 4417–4425, doi:10.1016/j.chroma.2011.05.020, 2011.

Kulmala, M., Kontkanen, J., Junninen, H., Lehtipalo, K., Manninen, H. E., Nieminen, T., Petäjä, T., Sipilä M., M., Schobesberger, S., Rantala, P., Franchin, A., Jokinen, T., Järvinen, E., Äijälä, M., Kangasluoma, J., Hakala, J., Aalto, P. P., Paasonen, P., Mikkilä, J., Vanhanen, J., Aalto, J., Hakola, H., Makkonen, U., Ruuskanen, T., Mauldin, R. L., Duplissy, J., Vehkamäki, H., Bäck, J., Kortelainen, A., Riipinen, I., Kurtén, T., Johnston, M. V, Smith, J. N., Ehn, M., Mentel, T. F., Lehtinen, K. E. J., Laaksonen, A., Kerminen, V.-M., and Worsnop, D. R.: Direct Observations of Atmospheric Aerosol Nucleation, Science, 339, 943–946, https://doi.org/10.1126/science.1227385, 2013.

Lelieveld, J.: Global Air Pollution Crossroads over the Mediterranean, Science, 298(5594), 794–799, doi:10.1126/science.1075457, 2002.

Li, Y., Pöschl, U., and Shiraiwa, M.: Molecular corridors and parameterizations of volatility in the chemical evolution of organic aerosols, Atmos. Chem. Phys., 16, 3327–3344, https://doi.org/10.5194/acp-16-3327-2016, 2016.

Liang, C., Pankow, J. F., Odum, J. R. and Seinfeld, J. H.: Gas/Particle Partitioning of Semivolatile Organic Compounds To Model Inorganic, Organic, and Ambient Smog Aerosols, Environ. Sci. Technol., 31(11), 3086–3092, doi:10.1021/es9702529, 1997.

Liggio, J., Li, S.-M. and McLaren, R.: Heterogeneous reactions of glyoxal on particulate matter : identification of acetals and sulfate esters, Environ. Sci. Technol., 39(6), 1532–1541, doi:10.1021/es048375y, 2005a.

Liggio, J., Li, S.-M. and McLaren, R.: Reactive uptake of glyoxal by particulate matter, J. Geophys. Res. Atmospheres, 110(D10), D10304, doi:10.1029/2004JD005113, 2005b.

Lim, Y. B., Tan, Y., Perri, M. J., Seitzinger, S. P. and Turpin, B. J.: Aqueous chemistry and its role in secondary organic aerosol (SOA) formation, Atmospheric Chem. Phys., 10(21), 10521–10539, doi:10.5194/acp-10-10521-2010, 2010.

Liu, F., Duan, F.-K., Li, H.-R., Ma, Y.-L., He, K.-B. and Zhang, Q.: Solid Phase Microextraction/Gas Chromatography-Tandem Mass Spectrometry for Determination of Polycyclic Aromatic Hydrocarbons in Fine Aerosol in Beijing, Chin. J. Anal. Chem., 43(4), 540–546, doi:10.1016/S1872-2040(15)60818-0, 2015.

Matsunaga, S.: Variation on the atmospheric concentrations of biogenic carbonyl compounds and their removal processes in the northern forest at Moshiri, Hokkaido Island in Japan, J. Geophys. Res., 109(D4), doi:10.1029/2003JD004100, 2004.

Michoud, V., Sciare, J., Sauvage, S., Dusanter, S., Léonardis, T., Gros, V., Kalogridis, C., Zannoni, N., Féron, A., Petit, J.-E., Crenn, V., Baisnée, D., Sarda-Estève, R., Bonnaire, N., Marchand, N., DeWitt, H. L., Pey, J., Colomb, A., Gheusi, F., Szidat, S., Stavroulas, I., Borbon, A., and Locoge, N.: Organic carbon at a remote site of the western Mediterranean Basin: sources and chemistry during the ChArMEx SOP2 field experiment, Atmos. Chem. Phys., 17, 8837–8865, https://doi.org/10.5194/acp-17-8837-2017, 2017.

Michoud, V., Sauvage, S., Léonardis, T., Fronval, I., Kukui, A., Locoge, N., and Dusanter, S.: Field measurements of methylglyoxal using proton transfer reaction time-of-flight mass spectrometry and comparison to the DNPH–HPLC–UV method, Atmos. Meas. Tech., 11, 5729–5740, https://doi.org/10.5194/amt-11-5729-2018, 2018.

Millán, M. M., Salvador, R., Mantilla, E. and Kallos, G.: Photooxidant dynamics in the Mediterranean basin in summer: Results from European research projects, J. Geophys. Res. Atmospheres, 102(D7), 8811–8823, doi:10.1029/96JD03610, 1997.

Minguillón, M. C., Ripoll, A., Pérez, N., Prévôt, A. S. H., Canonaco, F., Querol, X. and Alastuey, A.: Chemical characterization of submicron regional background aerosols in the western Mediterranean using an Aerosol Chemical Speciation Monitor, Atmospheric Chem. Phys., 15(11), 6379–6391, doi:10.5194/acp-15-6379-2015, 2015.

Moller, B., Rarey, J. and Ramjugernath, D.: Estimation of the vapour pressure of non-electrolyte organic compounds via group contributions and group interactions, J. Mol. Liq., 143(1), 52–63, doi:10.1016/j.molliq.2008.04.020, 2008.

Moroni, B., Castellini, S., Crocchianti, S., Piazzalunga, A., Fermo, P., Scardazza, F. and Cappelletti, D.: Ground-based measurements of long-range transported aerosol at the rural regional background site of Monte Martano (Central Italy), Atmospheric Res., 155, 26–36, doi:10.1016/j.atmosres.2014.11.021, 2015.

Myrdal, P. B. and Yalkowsky, S. H.: Estimating Pure Component Vapor Pressures of Complex Organic Molecules, Ind. Eng. Chem. Res., 36(6), 2494–2499, doi:10.1021/ie950242l, 1997.

Nannoolal, Y., Rarey, J., Ramjugernath, D. and Cordes, W.: Estimation of pure component properties: Part 1. Estimation of the normal boiling point of non-electrolyte organic compounds via group contributions and group interactions, Fluid Phase Equilibria, 226, 45–63, doi:10.1016/j.fluid.2004.09.001, 2004.

Nannoolal, Y., Rarey, J. and Ramjugernath, D.: Estimation of pure component properties: Part 3. Estimation of the vapor pressure of non-electrolyte organic compounds via group contributions and group interactions, Fluid Phase Equilibria, 269(1–2), 117–133, doi:10.1016/j.fluid.2008.04.020, 2008.

Ng, N. L., Canagaratna, M. R., Jimenez, J. L., Chhabra, P. S., Seinfeld, J. H. and Worsnop, D. R.: Changes in organic aerosol composition with aging inferred from aerosol mass spectra, Atmospheric Chem. Phys., 11(13), 6465–6474, doi:10.5194/acp-11-6465-2011, 2011.

Nguyen, T. B., Laskin, J., Laskin, A. and Nizkorodov, S. A.: Nitrogen-Containing Organic Compounds and Oligomers in Secondary Organic Aerosol Formed by Photooxidation of Isoprene, Environ. Sci. Technol., 45(16), 6908–6918, doi:10.1021/es201611n, 2011.

Nguyen, T. B., Nizkorodov, S. A., Laskin, A. and Laskin, J.: An approach toward quantification of organic compounds in complex environmental samples using high-resolution electrospray ionization mass spectrometry, Anal. Methods, 5(1), 72, doi:10.1039/c2ay25682g, 2013.

Nicolas, J. B.: Caractérisation physico-chimique de l'aérosol troposphérique en Méditerranée : sources et devenir, Université de Versailles Saint-Quentin-en-Yvelines (UVSQ). [online] Available from: http://www.uvsq.fr/caracterisation-physico-chimique-de-l-aerosol-tropospherique-en-mediterranee-sources-et-devenir-par-jose-nicolas-303880.kjsp (Accessed 2 February 2016), 2013.

Nozière, B., Kalberer, M., Claeys, M., Allan, J., D'Anna, B., Decesari, S., Finessi, E., Glasius, M., Grgić, I., Hamilton, J. F., Hoffmann, T., Iinuma, Y., Jaoui, M., Kahnt, A., Kampf, C. J., Kourtchev, I., Maenhaut, W., Marsden, N., Saarikoski, S., Schnelle-Kreis, J., Surratt, J. D., Szidat, S., Szmigielski, R. and Wisthaler, A.: The molecular identification of organic compounds in the atmosphere : state of the art and challenges, Chem. Rev., 150203102816008, doi:10.1021/cr5003485, 2015.

Orsini, D. A., Ma, Y., Sullivan, A., Sierau, B., Baumann, K. and Weber, R. J.: Refinements to the particle-into-liquid sampler (PILS) for ground and airborne measurements of water soluble aerosol composition, Atmos. Environ., 37(9–10), 1243–1259, doi:10.1016/S1352-2310(02)01015-4, 2003.

Pankow, J. F.: An absorption model of gas/particle partitioning of organic compounds in the atmosphere, Atmos. Environ., 28(2), 185–188, 1994.

Parshintsev, J. and Hyötyläinen, T.: Methods for characterization of organic compounds in atmospheric aerosol particles, Anal. Bioanal. Chem., 407(20), 5877–5897, doi:10.1007/s00216-014-8394-3, 2015.

Parshintsev, J., Rasanen, R., Hartonen, K., Kulmala, M. and Riekkola, M.-L.: Analysis of organic compounds in ambient aerosols collected with the particle-into-liquid sampler, Boreal Environ. Res., 14(4), 630–640, 2009.

Pietrogrande, M. C., Bacco, D. and Mercuriali, M.: GC–MS analysis of low-molecular-weight dicarboxylic acids in atmospheric aerosol: comparison between silylation and esterification derivatization procedures, Anal. Bioanal. Chem., 396(2), 877–885, doi:10.1007/s00216-009-3212-z, 2009.

Pöschl, U.: Atmospheric Aerosols : composition, transformation, climate and health effects, Angew. Chem. Int. Ed., 44(46), 7520–7540, doi:10.1002/anie.200501122, 2005.

Querol, X., Pey, J., Pandolfi, M., Alastuey, A., Cusack, M., Pérez, N., Moreno, T., Viana, M., Mihalopoulos, N., Kallos, G. and Kleanthous, S.: African dust contributions to mean ambient PM10 mass-levels across the Mediterranean Basin, Atmos. Environ., 43(28), 4266–4277, doi:10.1016/j.atmosenv.2009.06.013, 2009a.

Querol, X., Alastuey, A., Pey, J., Cusack, M., Pérez, N., Mihalopoulos, N., Theodosi, C., Gerasopoulos, E., Kubilay, N. and Koçak, M.: Variability in regional background aerosols within the Mediterranean, Atmos Chem Phys, 9(14), 4575–4591, doi:10.5194/acp-9-4575-2009, 2009b.

Raventos-Duran, T., Camredon, M., Valorso, R., Mouchel-Vallon, C. and Aumont, B.: Structure-activity relationships to estimate the effective Henry's law constants of organics of atmospheric interest, Atmos Chem Phys, 10(16), 7643–7654, doi:10.5194/acp-10-7643-2010, 2010.

Ripoll, A., Minguillón, M. C., Pey, J., Pérez, N., Querol, X. and Alastuey, A.: Joint analysis of continental and regional background environments in the western Mediterranean: PM1 and PM10 concentrations and composition, Atmospheric Chem. Phys., 15(2), 1129–1145, doi:10.5194/acp-15-1129-2015, 2015.

Robinson, A. L., Donahue, N. M., Shrivastava, M. K., Weitkamp, E. A., Sage, A. M., Grieshop, A. P., Lane, T. E., Pierce, J. R. and Pandis, S. N.: Rethinking organic aerosols : semivolatile emissions and photochemical aging, Science, 315(5816), 1259–1262, doi:10.1126/science.1133061, 2007.

Rossignol, S.: Développement d'une méthode de prélèvement simultané et d'analyse chimique des phases gazeuse et particulaire atmosphériques pour une approche multiphasique de l'aérosol

organique secondaire, Paris 7. [online] Available from: http://www.theses.fr/2012PA077208 (Accessed 14 February 2016), 2012.

Rossignol, S., Chiappini, L., Perraudin, E., Rio, C., Fable, S., Valorso, R. and Doussin, J. F.: Development of a parallel sampling and analysis method for the elucidation of gas/particle partitioning of oxygenated semi-volatile organics: a limonene ozonolysis study, Atmospheric Meas. Tech., 5(6), 1459–1489, doi:10.5194/amt-5-1459-2012, 2012.

Rossignol, S., Couvidat, F., Rio, C., Fable, S., Grignion, G., Savelli, Pailly, O., Leoz-Garziandia, E., Doussin, J.-F. and Chiappini, L.: Organic aerosol molecular composition and gas–particle partitioning coefficients at a Mediterranean site (Corsica), J. Environ. Sci., 40, 92–104, doi:10.1016/j.jes.2015.11.017, 2016.

Samake A, Jaffrezo JL, Favez O, Weber S, Jacob V, Albinet A, Riffault V, Perdrix E, Waked A, Golly B, Salameh D, Chevrier F, Oliveira D, Bonnaire N, Besombes JL, Martins JMF, Conil S, Guillaud G, Mesbah B, Rocq B, Robic PY, Hulin A, Le Meur S, Descheemaecker M, Chretien E, Marchand N, and Uzu G. (2019) Polyols and Glucose Particulate Species as Tracers of Primary Biogenic Organic Aerosols at 28 French Sites. Atmos. Chem. Phys., doi.org/10.5194/acp-19-3357-2019.

Schoene, K., Bruckert, H.-J., Steinhanses, J. and König, A.: Two stage derivatization with N-(tert.-butyldimethylsilyl)-N-methyl-trifluoroacetamide (MTBSTFA) and N-methyl-bis-(trifluoroacetamide)(MBTFA) for the gas-chromatographic analysis of OH-, SH-and NH-compounds, Fresenius J. Anal. Chem., 348(5-6), 364–370, 1994.

Sciare, J., d'Argouges, O., Sarda-Estève, R., Gaimoz, C., Dolgorouky, C., Bonnaire, N., Favez, O., Bonsang, B. and Gros, V.: Large contribution of water-insoluble secondary organic aerosols in the region of Paris (France) during wintertime, J. Geophys. Res. Atmospheres, 116(D22), D22203, doi:10.1029/2011JD015756, 2011.

Seinfeld, J. H. and Pankow, J. F.: Organic atmospheric particulate material, Annu. Rev. Phys. Chem., 54(1), 121–140, doi:10.1146/annurev.physchem.54.011002.103756, 2003.

Shiraiwa, M., Ammann, M., Koop, T. and Pöschl, U.: Gas uptake and chemical aging of semisolid organic aerosol particles, Proc. Natl. Acad. Sci., 108(27), 11003–11008, 2011.

Shrivastava, M. K., Subramanian, R., Rogge, W. F. and Robinson, A. L.: Sources of organic aerosol : positive matrix factorization of molecular marker data and comparison of results from different source apportionment models, Atmos. Environ., 41(40), 9353–9369, doi:10.1016/j.atmosenv.2007.09.016, 2007.

Soonsin, V., Zardini, A. A., Marcolli, C., Zuend, A. and Krieger, U. K.: The vapor pressures and activities of dicarboxylic acids reconsidered: the impact of the physical state of the aerosol, Atmos Chem Phys, 10(23), 11753–11767, doi:10.5194/acp-10-11753-2010, 2010.

Sorooshian, A., Brechtel, F. J., Ma, Y. L., Weber, R. J., Corless, A., Flagan, R. C., and Seinfeld, J. H.: Modeling and characterization of a particle-into-liquid sampler (PILS), Aerosol Sci. Tech., 40, 396–409, 2006.

Srivastava, D., Tomaz, S., Favez, O., Lanzafame, G. M., Golly, B., Besombes, J.-L., Alleman, L. Y., Jaffrezo, J.-L., Jacob, V., Perraudin, E., Villenave, E., and Albinet, A.: Speciation of organic fraction does matter for source apportionment. Part 1: A one-year campaign in Grenoble (France), Sci. Total Environ., 624, 1598– 1611, 2018

Tolocka, M. P., Jang, M., Ginter, J. M., Cox, F. J., Kamens, R. M. and Johnston, M. V.: Formation of oligomers in secondary organic aerosol, Environ. Sci. Technol., 38(5), 1428–1434, doi:10.1021/es035030r, 2004.

Valach, A. C., Langford, B., Nemitz, E., MacKenzie, A. R. and Hewitt, C. N.: Concentrations of selected volatile organic compounds at kerbside and background sites in central London, Atmos. Environ., 95, 456–467, doi:10.1016/j.atmosenv.2014.06.052, 2014.

van Drooge, B. L., Nikolova, I. and Ballesta, P. P.: Thermal desorption gas chromatography–mass spectrometry as an enhanced method for the quantification of polycyclic aromatic hydrocarbons from ambient air particulate matter, J. Chromatogr. A, 1216(18), 4030–4039, doi:10.1016/j.chroma.2009.02.043, 2009.

Virtanen, A., Joutsensaari, J., Koop, T., Kannosto, J., Yli-Pirilä, P., Leskinen, J., Mäkelä, J. M., Holopainen, J. K., Pöschl, U., Kulmala, M., Worsnop, D. R. and Laaksonen, A.: An amorphous solid state of biogenic secondary organic aerosol particles, Nature, 467(7317), 824–827, doi:10.1038/nature09455, 2010.

Washenfelder, R. A., Young, C. J., Brown, S. S., Angevine, W. M., Atlas, E. L., Blake, D. R., Bon, D. M., Cubison, M. J., de Gouw, J. A., Dusanter, S., Flynn, J., Gilman, J. B., Graus, M., Griffith, S., Grossberg, N., Hayes, P. L., Jimenez, J. L., Kuster, W. C., Lefer, B. L., Pollack, I. B., Ryerson, T. B., Stark, H., Stevens, P. S., and Trainer, M. K.: The glyoxal budget and its contribution to organic aerosol for Los Angeles, California, during CalNex 2010, J. Geophys. Res., 116, D00V02, https://doi.org/10.1029/2011JD016314, 2011

Williams, B. J., Goldstein, A. H., Kreisberg, N. M. and Hering, S. V.: An In-Situ Instrument for Speciated Organic Composition of Atmospheric Aerosols: Thermal Desorption Aerosol GC/MS-FID (TAG), Aerosol Sci. Technol., 40(8), 627–638, doi:10.1080/02786820600754631, 2006.

Woody, M. C., Baker, K. R., Hayes, P. L., Jimenez, J. L., Koo, B., and Pye, H. O. T.: Understanding sources of organic aerosol during CalNex-2010 using the CMAQ-VBS, Atmos. Chem. Phys., 16, 4081–4100, https://doi.org/10.5194/acp-16-4081-2016, 2016.

Zannoni, N., Gros, V., Sarda Esteve, R., Kalogridis, C., Michoud, V., Dusanter, S., Sauvage, S., Locoge, N., Colomb, A., and Bonsang, B.: Summertime OH reactivity from a receptor coastal site in the Mediterranean Basin, Atmos. Chem. Phys., 17, 12645–12658, https://doi.org/10.5194/acp-17-12645-2017, 2017.

Zhang, H., Surratt, J. D., Lin, Y. H., Bapat, J. and Kamens, R. M.: Effect of relative humidity on SOA formation from isoprene/NO photooxidation : enhancement of 2-methylglyceric acid and its corresponding oligoesters under dry conditions, Atmospheric Chem. Phys., 11(13), 6411–6424, doi:10.5194/acp-11-6411-2011, 2011.

Zhang, X., Dalleska, N. F., Huang, D. D., Bates, K. H., Sorooshian, A., Flagan, R. C. and Seinfeld, J. H.: Time-resolved molecular characterization of organic aerosols by PILS + UPLC/ESI-Q-TOFMS, Atmos. Environ., 130, 180–189, doi:10.1016/j.atmosenv.2015.08.049, 2016.

Zobrist, B., Soonsin, V., Luo, B. P., Krieger, U. K., Marcolli, C., Peter, T. and Koop, T.: Ultra-slow water diffusion in aqueous sucrose glasses, Phys. Chem. Chem. Phys., 13(8), 3514–3526, doi:10.1039/C0CP01273D, 2011.

1 Table 1: Thermal desorption method and GC/MS parameters

Thermal desorption parameters for samples	temperature	300°C
	time	15 minutes
	flow	50 mL min^{-1}
	split flow	No split flow
Thermal desorption parameters for the trap	Temperature	From -10°C to 300°C
	Time	12 minutes
	flow	10 mL min^{-1}
Temperature of transfer lines		200°C
GC Parameters	Carrier gas	He
	Carrier gas flow	1 mL min^{-1}
	Temperature gradient	40°C / 10°C min^{-1} / 305°C (10 min)
	Split flow	0.2 mL min^{-1}
	Transfer line temperature to MS	305 °C
MS parameters	Scan m/z	40 to 800
	Solvent delay	5 min
	Quadrupole temperature	150°C
	EI -Source temperature -Ionization Energy	 230°C 70 eV
	CI -Source temperature -Reagent gas -Ionization Energy	 250°C CH_4 50 eV

2

3

1 Table 2 : List of substitutes used for internal calibration

Substitutes used for carbonyl compounds	**Substitutes used for hydroxyl compounds**
3-methylbutanal-d2	Pentanoic acid-d9
Butanal-d8	Heptanoic acid-d13
4-methyl-2-pentanone-d5	Succinic acid-d4
Benzaldehyde-d6	2-methyl-d3-2-propyl-1,3-propanediol
Acetophenone-d8	Glycerol-d8
2-hexanone-d5	Tartaric acid-2,3-d2
2,3-butanedione-d5	
2,5-hexanedione-d10	

2

3

Table 3: meteorological conditions, environmental parameters and mass concentrations of PM_{10}, PM_1 and organic fraction in PM_1 during the ChArMEx campaign at ERSA

Meteorological and Environmental Parameters	**Mean**	**Median**	**Max**	**Min**
Temperature (°C)	23	23	32	19
Relative Humidity (%)	70	73	100	27
Wind Speed (m s^{-1})	3.6	3.1	13.2	-
O_3 (ppbv)	65	65	111	42
NO_x (ppbv)	0.57	0.45	4.93	0.06
Mass concentrations (µg m^{-3})	**Mean (±1σ)**	**Median**	**Max**	**Min**
PM_{10}	12 (±4.8)	12	31	2
PM_1	8.4 (±4.4)	8.4	22	0.2
Organic fraction (PM_1)	3.7 (±1.7)	3.5	8.1	0.2

Table 4: Experimental (averaged over the campaign with ±XX% representing 1σ standard deviation over the campaign) and theoretical partitioning coefficients determined for this study and compared to previous field and chamber campaigns.

	This study	Corsica [a]	EuPhoRe [a]	Kpt,i MOL [b]	Kpt,i NAN [c]	Kpt,i MYR [d]
Propanal	$6.1x10^{-3}$ ± 75 %	$2.2x10^{-3}$ ± 50 %		$2.6x10^{-10}$	$2.6x10^{-10}$	$4.7x10^{-10}$
Pentanal	$6.5x10^{-4}$ ± 106 %**	$1.8x10^{-4}$ ± 51 %		$3.2x10^{-9}$	$3.2x10^{-9}$	$3.8x10^{-9}$
Hexanal	$1.3x10^{-3}$ ± 61 %			$1.0x10^{-8}$	$1.0x10^{-8}$	$1.1x10^{-8}$
Heptanal	$5.1x10^{-4}$ ± 91 %			$3.3x10^{-8}$	$3.2x10^{-8}$	$3.4x10^{-8}$
Acrolein	$7.3x10^{-4}$ ± 74 %	$6.1x10^{-3}$ ± 50 %		$3.6x10^{-10}$	$3.6x10^{-10}$	$3.7x10^{-7}$
Methacrolein	$7.3x10^{-4}$ ± 69 %			$7.2x10^{-10}$	$7.2x10^{-10}$	$9.0x10^{-10}$
Methyl Vinyl ketone	$5.8x10^{-4}$ ± 57 %			$1.3x10^{-9}$	$1.3x10^{-9}$	$5.6x10^{-10}$
Nopinone	$5.5x10^{-4}$ ± 53 %			$1.7x10^{-7}$	$1.7x10^{-7}$	$1.9x10^{-7}$
Dimethylglyoxal	$5.0x10^{-3}$ ± 65 %	$5.6x10^{-4}$ ± 70 %	$6.2x10^{-4}$ ± 47 %		$3.4x10^{-9}$ *	$7.0x10^{-9}$ *
Methylglyoxal	$3.6x10^{-3}$ ± 60 %	$2.2x10^{-2}$ ± 132 %**	$1.3x10^{-3}$ ± 84 %		$8.6x10^{-10}$ *	$2.1x10^{-9}$ *
Levulinic acid	$5.1x10^{-3}$ ± 77 %			$1.7x10^{-5}$	$4.4x10^{-6}$	$2.9x10^{-6}$
Methacrylic acid	$1.5x10^{-4}$ ± 198 %**			$8.4x10^{-8}$	$7.6x10^{-8}$	$8.9x10^{-8}$
Glycolic acid	$3.1x10^{-2}$ ± 268 %**			$8.5x10^{-5}$	$1.3x10^{-5}$	$2.0x10^{-6}$
Glycerol	$1.1x10^{-2}$ ± 62 %			$7.1x10^{-4}$	$8.4x10^{-4}$	$1.3x10^{-5}$

[a] Rossignol et al., 2016; [b] Moller et al., 2008 (coupled with Nannoolal et al. (2004) method for boiling point determination) ; [c] Nannoolal et al., 2008 (coupled with Nannoolal et al. (2004) method for boiling point determination) ; [d] Myrdal and Yalkowsky, 1997 (coupled with Nannoolal et al. (2004) method for boiling point determination)

* Coefficients extracted from Rossignol, 2012 at temperature of 300 K other parameter (MW_{om} et ζ_i) kept similar.

** Partitioning coefficients are comprised between 0 and 1. Experimental uncertainties greater than 100% mean that the experimental value is comprised between 0 and more than twice its values.

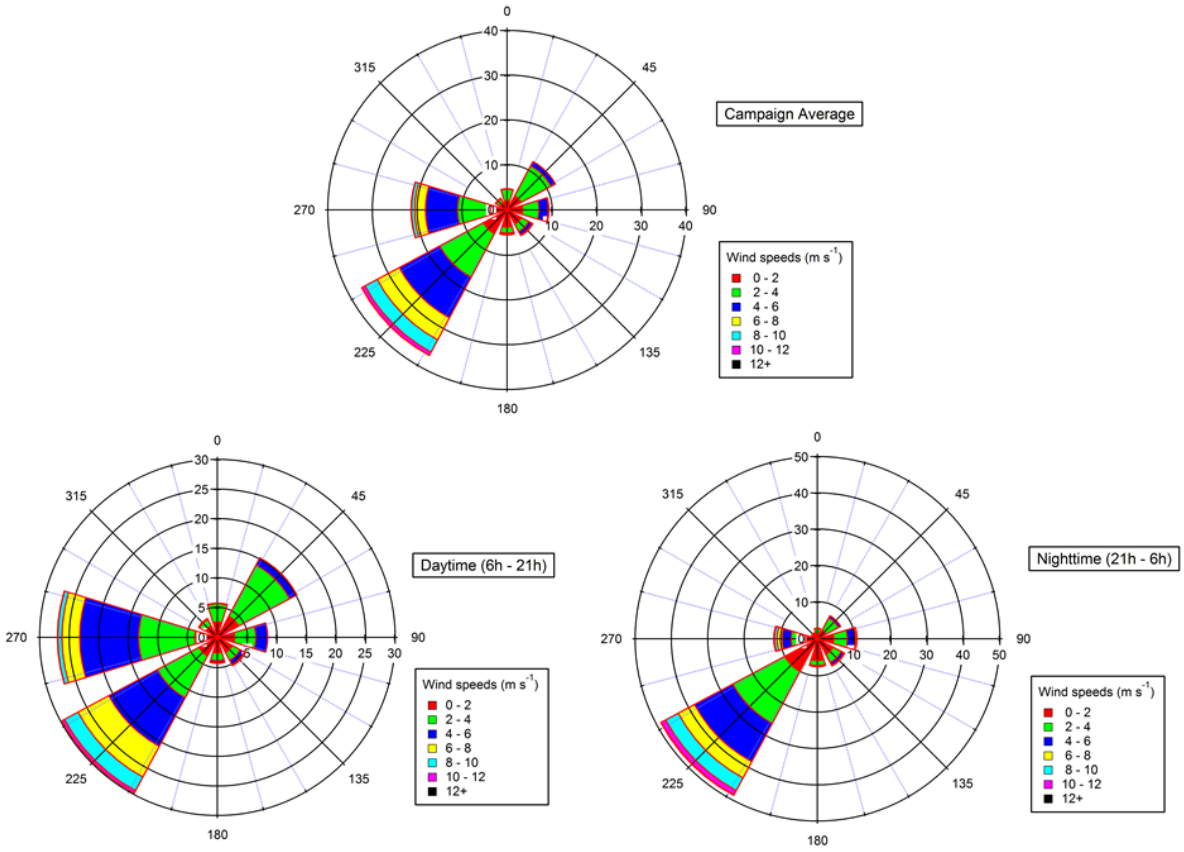

1

2 Figure 1 : Wind roses from July 15th to August 5th 2013 (top panel), during daytime only (bottom left
3 panel) and during nighttime only (bottom right panel). Wind direction is expressed in ° and radial axe
4 express the relative occurrence of wind in each 30° sector (%).

5

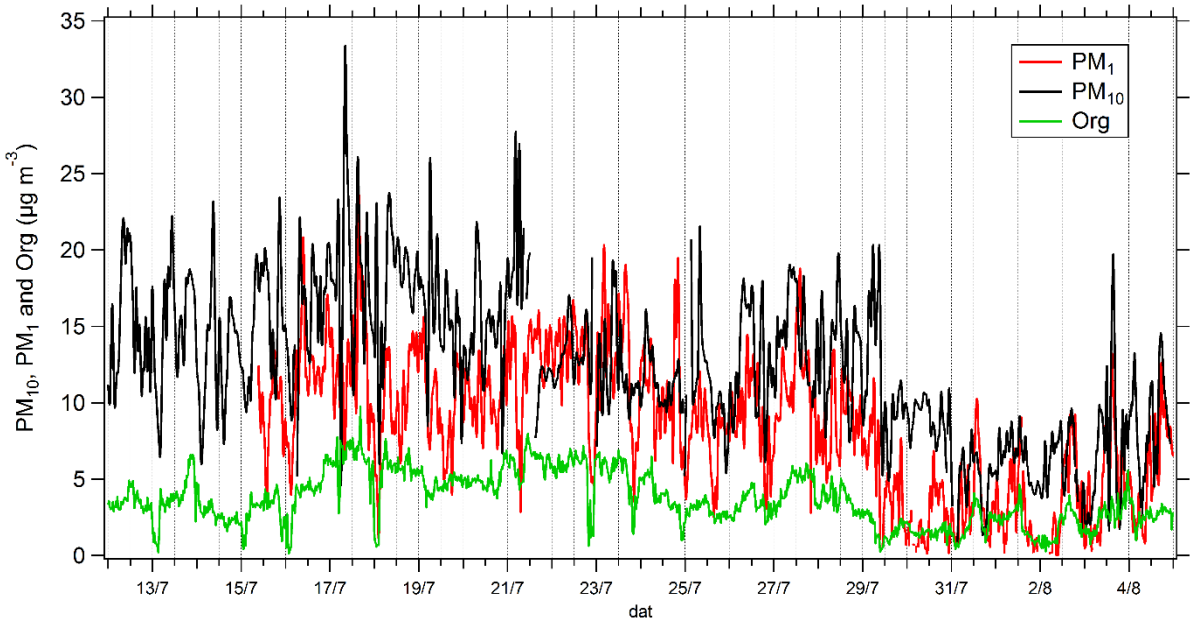

Figure 2 : Time series of mass concentrations of PM_{10} (black line), PM_1 (red line) and organic fraction in NR-PM_1 (green line).

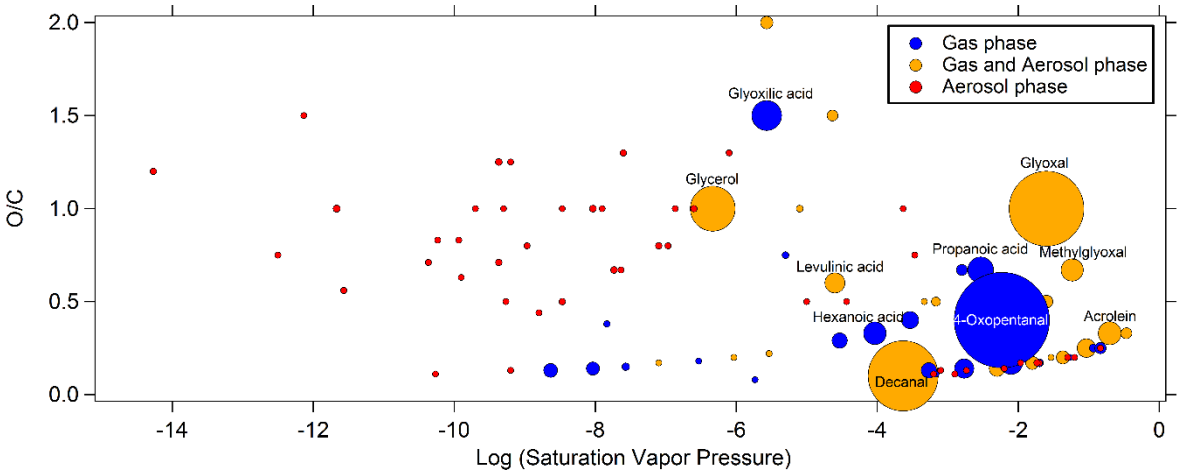

Figure 3: Distribution of compounds identified by TD-GC/MS during the ChArMEx campaign according to the logarithm of their saturation vapor pressure (horizontal axis) and of their O/C ratio (vertical axis). The phase in which they are detected is color-coded: blue for compounds only detected in the gas phase, red for aerosol phase only and orange for compounds detected in both phases. Each dot represents a single compound and the dot area is proportional to the sum of concentrations if detected in both phases from 0.3 ng m^{-3} for the smallest dot to 3.9 µg m^{-3} for the biggest one. Name of some noticeable compounds are also given.

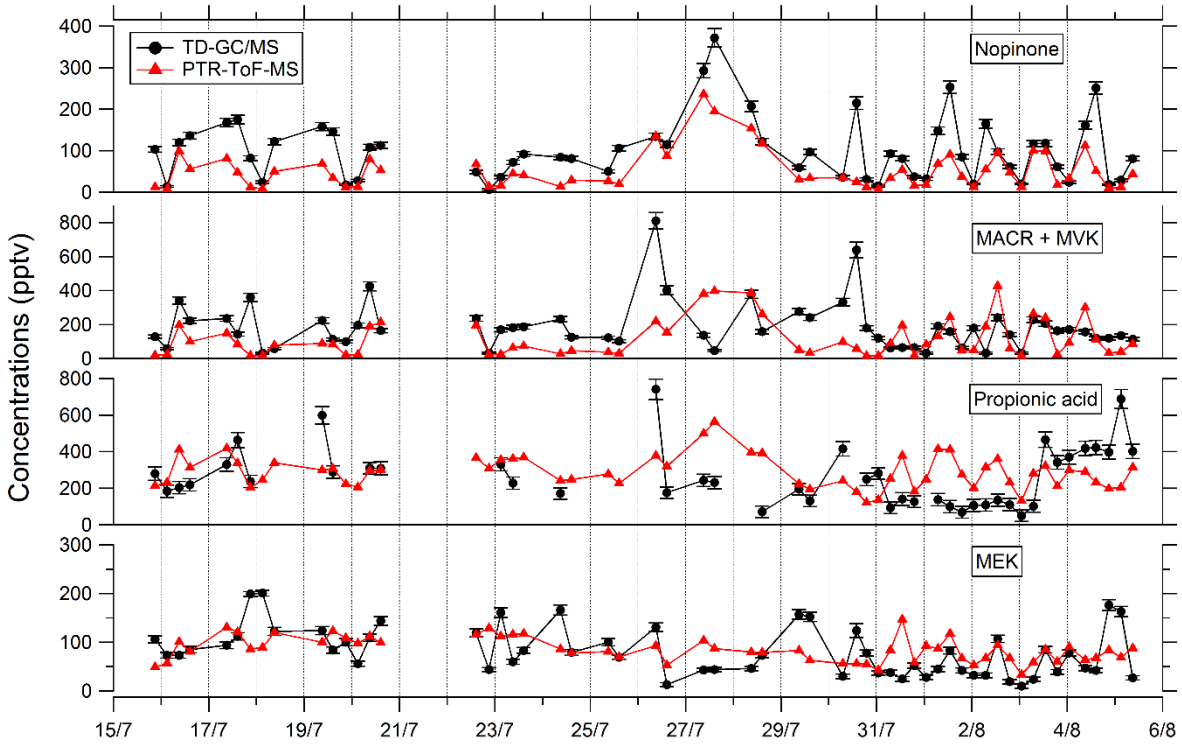

Figure 4 : Comparison of ATD-GC-MS data with PTR-ToF-MS data averaged over the same time step for nopinone, the sum of methacrolein and methyl vinyl ketone, propionic acid and methyl ethyl ketone. Error bars correspond to the 1σ uncertainties of TD-GC/MS measurements. Error bars correspond to the 1σ uncertainties of TD-GC/MS measurements.

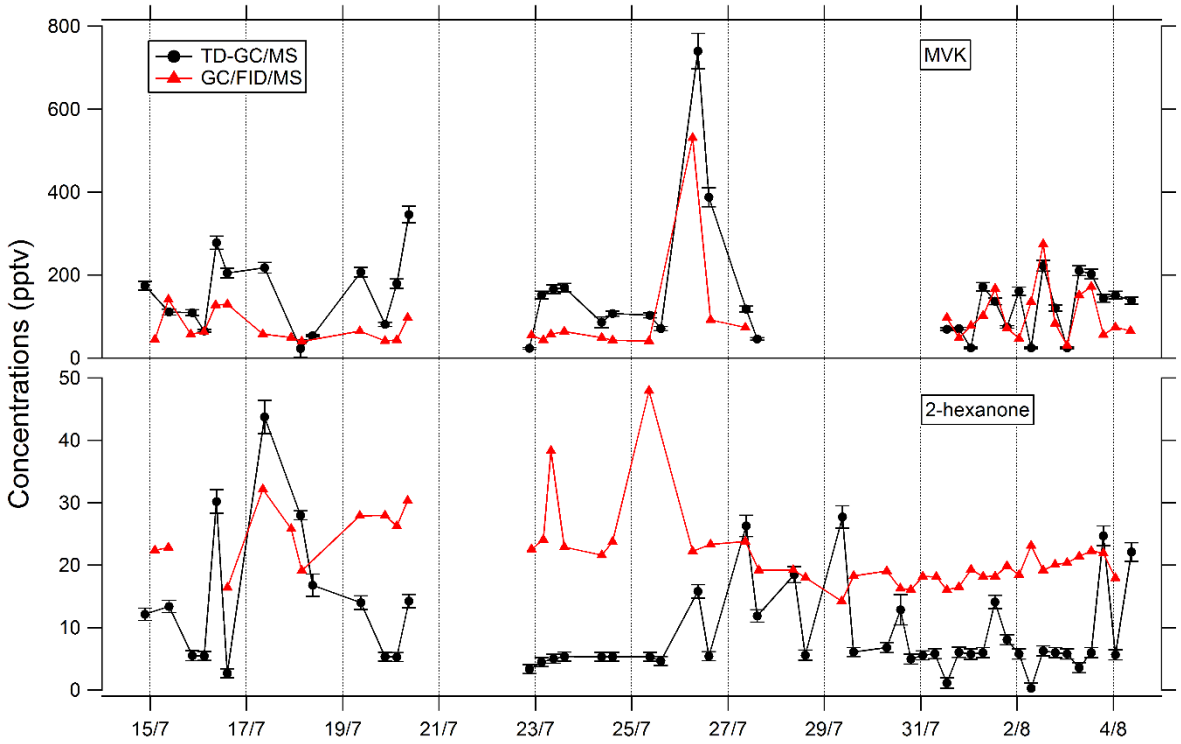

Figure 5 : Comparison of ATD-GC-MS data with GC/FID/MS data averaged over the same time step for methyl vinyl ketone and 2-hexanone. Error bars correspond to the 1σ uncertainties of TD-GC/MS measurements. Error bars correspond to the 1σ uncertainties of TD-GC/MS measurements.

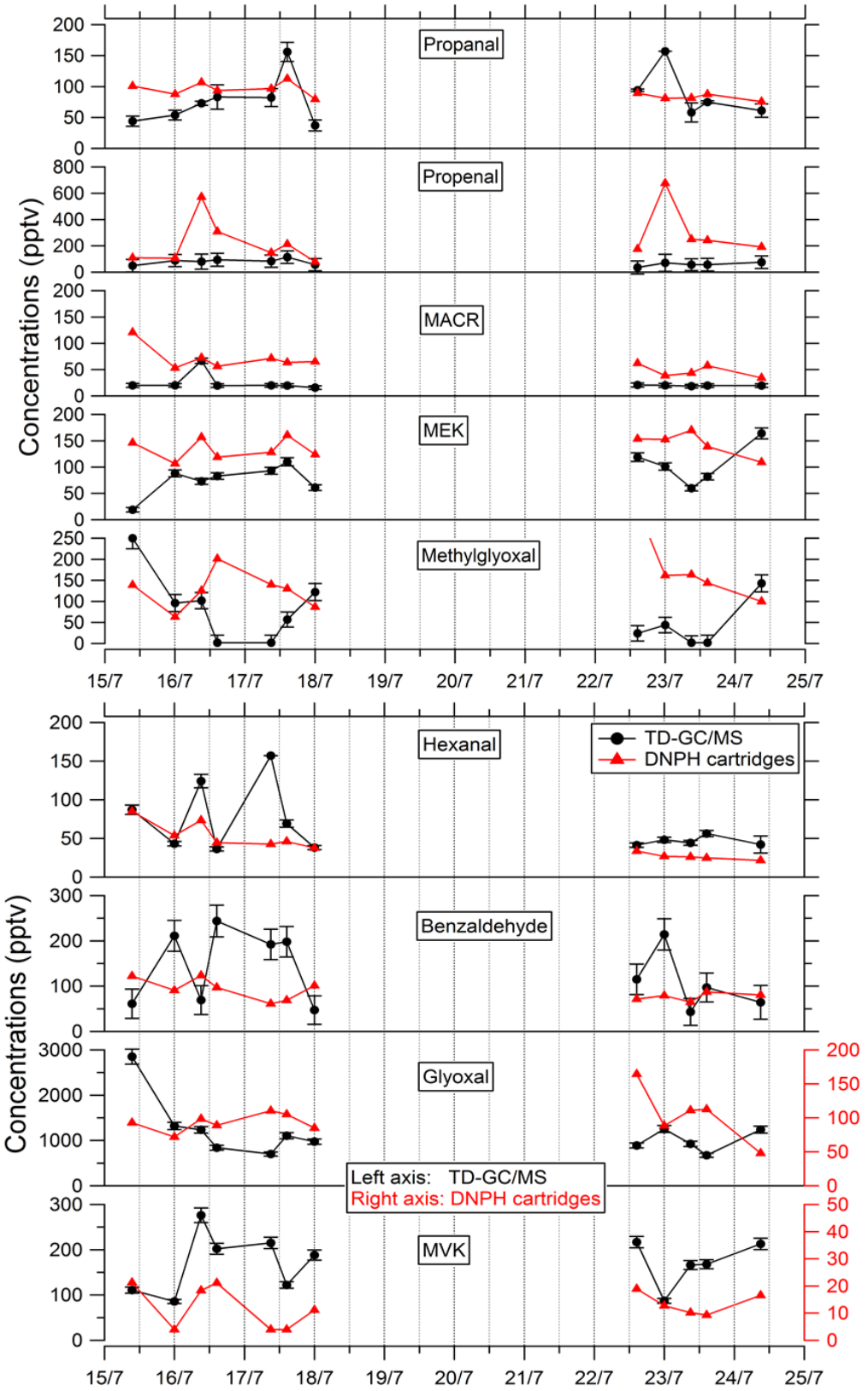

Figure 6 : Comparison of ATD-GC-MS data with DNPH cartridges analysis for 9 OVOCs. Error bars correspond to the 1σ uncertainties of TD-GC/MS measurements. Error bars correspond to the 1σ uncertainties of TD-GC/MS measurements.

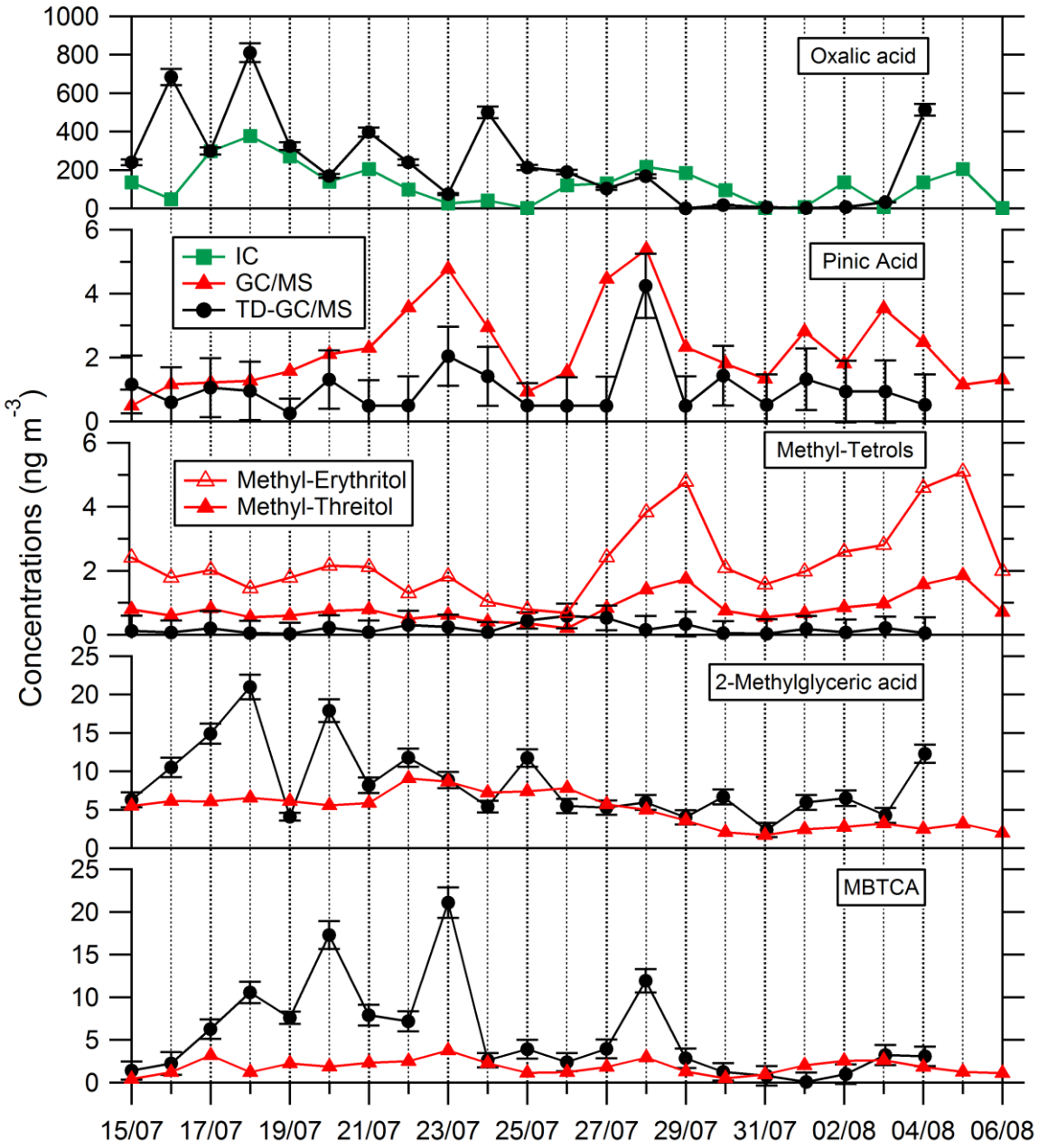

Figure 7 : Comparison of ATD-GC-MS data with ion chromatography and GC/MS analysis for particulate oxalic acid, pinic acid, methyl tetrols, 2-methylglyceric acid and MBTCA (3-Methyl-1,2,3-tricarboxylic acid). Error bars correspond to the 1σ uncertainties of TD-GC/MS measurements. Error bars correspond to the 1σ uncertainties of TD-GC/MS measurements.

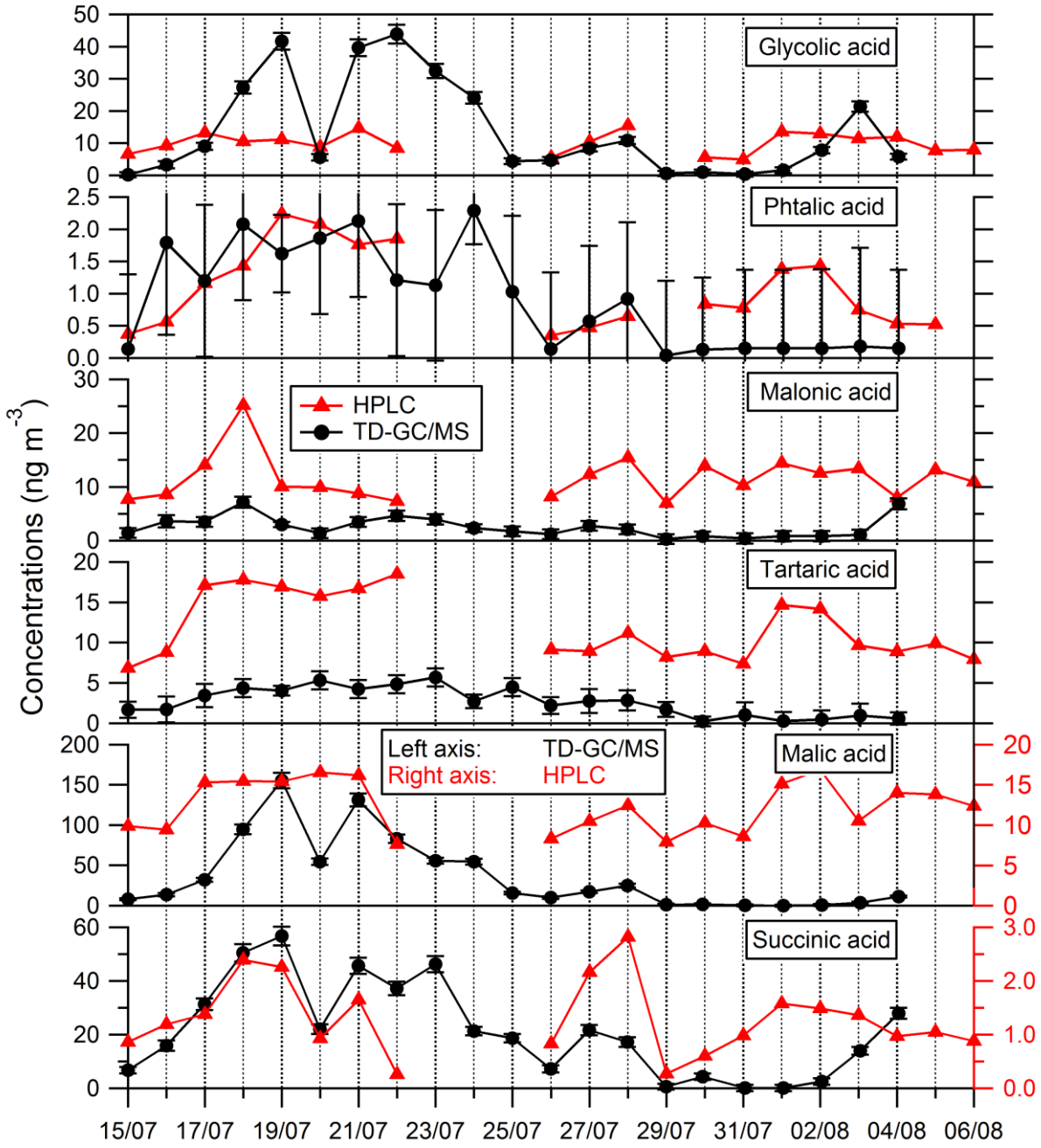

Figure 8: Comparison of ATD-GC-MS data with HPLC analysis for particulate glycolic acid, phtalic acid, malonic acid, tartaric acid, malic acid and succinic acid. Error bars correspond to the 1σ uncertainties of TD-GC/MS measurements. Error bars correspond to the 1σ uncertainties of TD-GC/MS measurements.

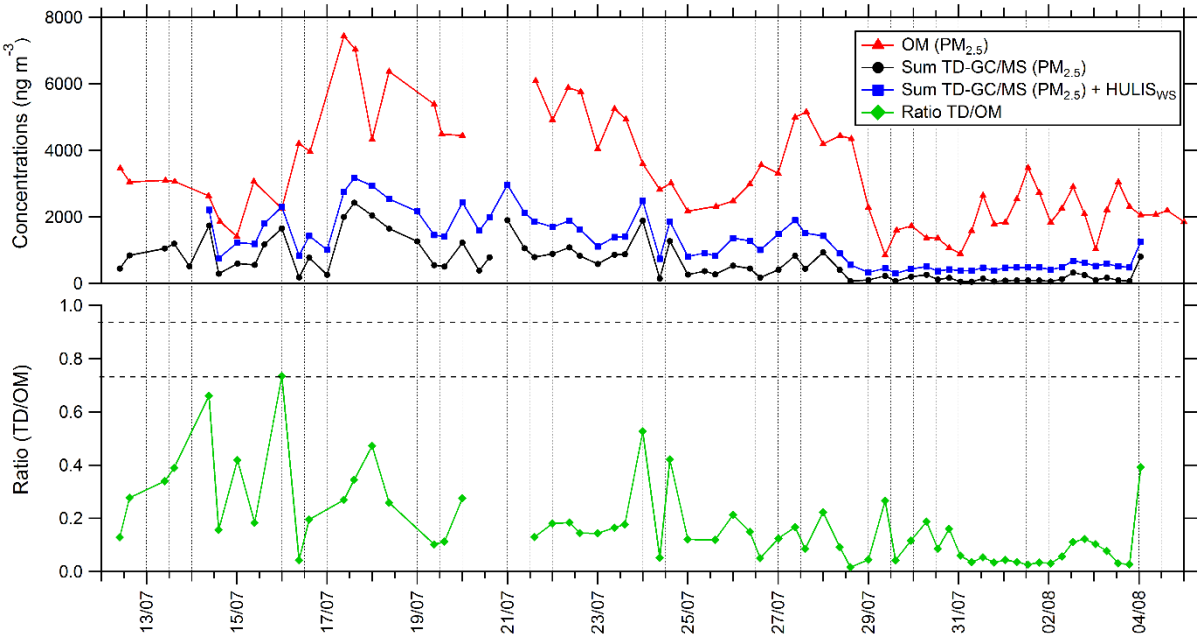

Figure 9: Time series of organic matter in $PM_{2.5}$ (red line), total sum of $PM_{2.5}$ from TD-GC/MS analysis (black line), total sum of $PM_{2.5}$ from TD-GC/MS analysis and water soluble HULIS analysis (blue line), and ratio of these two measurements (green line).

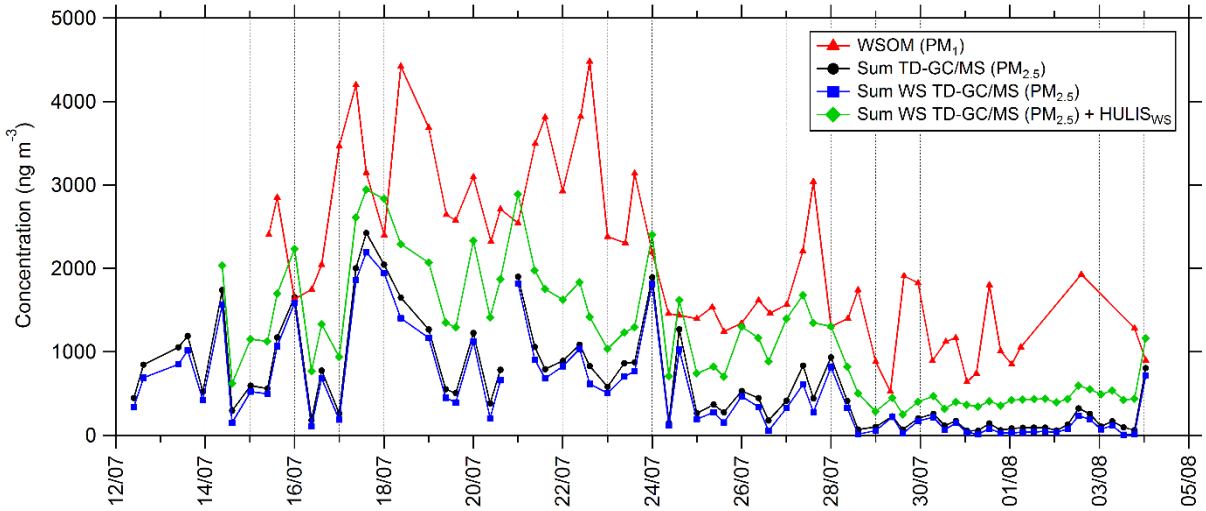

Figure 10: Time series of PM_1 water soluble organic matter (WSOM; red line), total sum of $PM_{2.5}$ measured by TD-GC/MS (black line), total sum of compounds measured by TD-GC/MS and having henry's law constant higher than 10^4 M atm^{-1} measured by TD-GC/MS (WS TD-GC/MS, blue line), and total sum of water soluble compounds measured by TD-GC/MS and water soluble HULIS (green line).

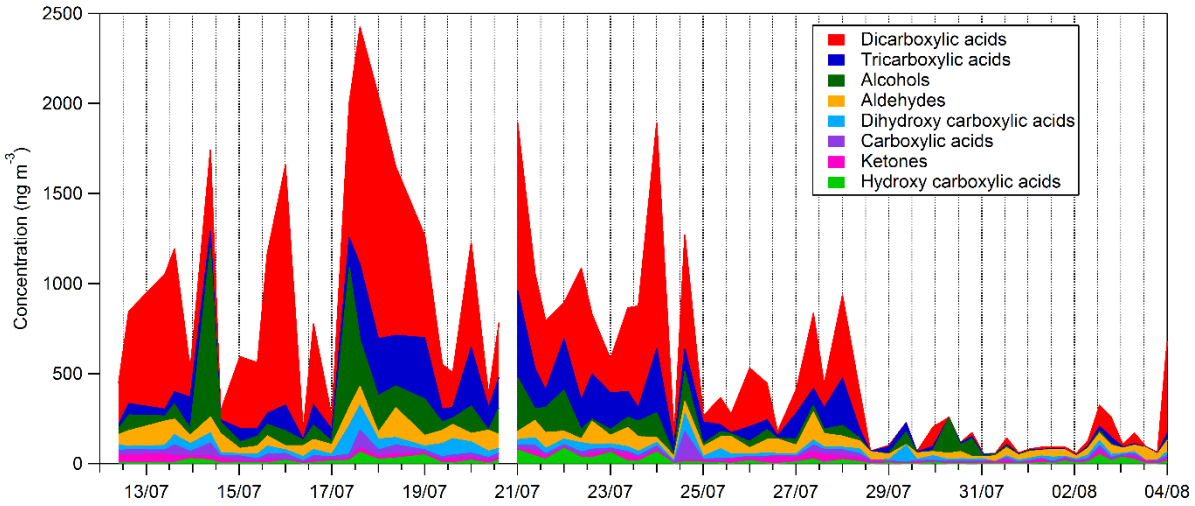

Figure 11: Time series of the composition of the sum of all compounds concentrations measured by TD-GC/MS.

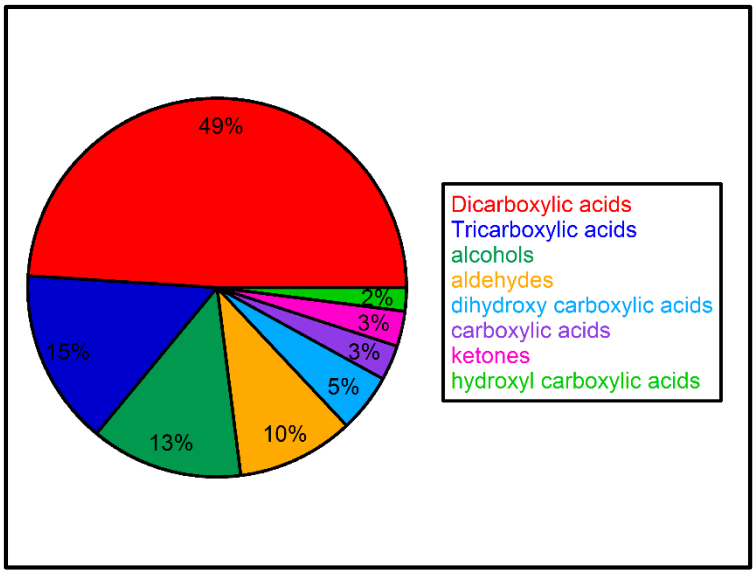

Figure 12: Campaign averaged relative composition of the sum of all compounds measured by TD-GC/MS in the organic aerosol phase (hydroxyl-carboxylic acid-light green area, ketone-pink area, carboxylic acid-purple area, dihydroxy carboxylic acid-light blue area, aldehyde-orange area, alcohol-dark green area, tricarboxylic acid-dark blue area, dicarboxylic acid-red area).

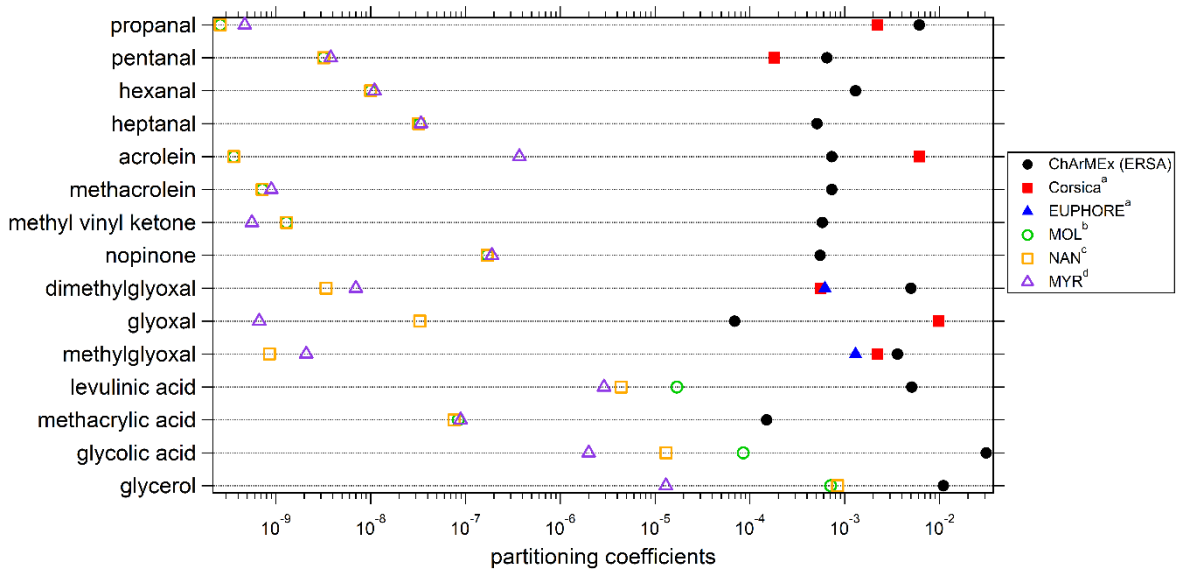

[a] Rossignol et al., 2016; [b] Moller et al., 2008 (coupled with Nannoolal et al. (2004) method for boiling point determination) ; [c] Nannoolal et al., 2008 (coupled with Nannoolal et al. (2004) method for boiling point determination) ; [d] Myrdal and Yalkowsky, 1997 (coupled with Nannoolal et al. (2004) method for boiling point determination)

Figure 13: Experimental and theoretical partitioning coefficients determined for this study and compared to previous field and chamber campaigns.